Макрогетероциклы
http://macroheterocycles.isuct.ru

Synthesis, Properties, and Potential Applications of Porphyrin–Fullerenes

Andrey F. Mironov

Lomonosov Moscow State University of Fine Chemical Technologies, 119571 Moscow, Russian Federation
E-mail: mironov@mitht.ru

Contents

The review focuses current research in the rapidly developing chemistry of porphyrin-fullerene complexes, and highlights recent advances in the synthesis, properties, and potential applications of this family. An overview of the most popular methods to prepare porphyrin complexes with C_{60} fullerene exhibiting various types of linkage is given with the main focus on the Prato reaction and its modifications. The discussion of porphyrin-fullerene complexes will include the structures of noncovalently linked porphyrin-fullerenes along with the covalently linked complexes; the chemistry and design of supramolecular ensembles will be covered rather comprehensively. Finally, the potential applications for porphyrin-fullerene conjugates will be discussed.

Keywords: Porphyrin-fullerenes, synthesis, Prato reaction, molecular constructs, application.

1. Introduction

Fullerene, a new allotrope of carbon previously found in the form of graphite, diamond, and amorphous carbon such as soot and charcoal was discovered by R. Smalley, R. Curl, and G. Croto in the mid-1980s. This discovery was awarded the Nobel Prize in Chemistry 1996, 11 years after the first report by its authors in 1985 in *Nature*.[1] The most recently discovered allotrope of carbon is graphene. The scientific community recognized the significance of this material much faster: Russian-born scientists Andre Geim and Konstantin Novoselov won the Nobel Prize in physics 2010 for their "groundbreaking experiments". However it was the discovery of fullerenes (whose size is of the order of 10^{-9} m which is actually “nano”) that gave a whole new insight into carbon materials. It all the rapid growth of nanomaterials and technology follows thereafter.

In a C_{60} fullerene, the carbon atoms link together into a soccer-ball-shaped cage with a surface formed by 12 pentagons and 20 hexagons with the carbon atoms sitting in the vertices of this polyhedron (namely, truncated icosahedron from Greek eikosaedron, from eikosi 'twenty' + hedra 'base').

All the later discovered fullerenes (presently the structures composed of > 100 carbon atoms are known) have the same 12 right pentagonal faces as in the first C_{60} fullerene, and $m = (n - 20)/2$ hexagonal faces, where n is the number of carbon atoms in the fullerene. Of this family, fullerenes composed of 60 and 70 carbons, C_{60} and C_{70}, are the most abundant.

Fullerenes have since been found to occur in nature. In the 1990s, fullerenes were identified in soot and coal, in Precambrian Karelian shungite (in up to 10 % concentrations) and even, more recently, in outer space.

Implemented by the advances in synthesis methods of fullerenes, the increased availability of fullerenes and fullerene-based products has resulted in their growing application in material science and nanotechnology engineering, particularly, as composite fibers in polymers, in semiconductors and superconductors, transistors, solar cells, in tissue engineering (medicine), *etc*.

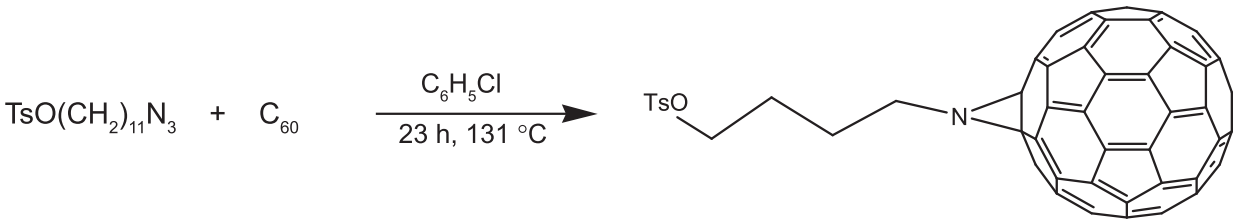

Scheme 1. Condensation of alkyl azides with C_{60} fullerene.

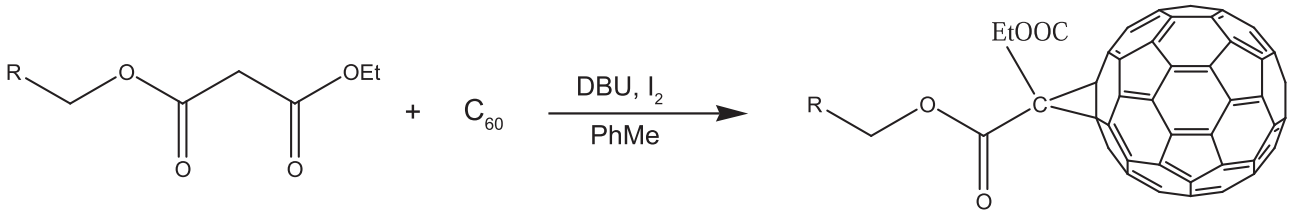

Scheme 2. Functionalization of C_{60} using malonic acid derivatives.

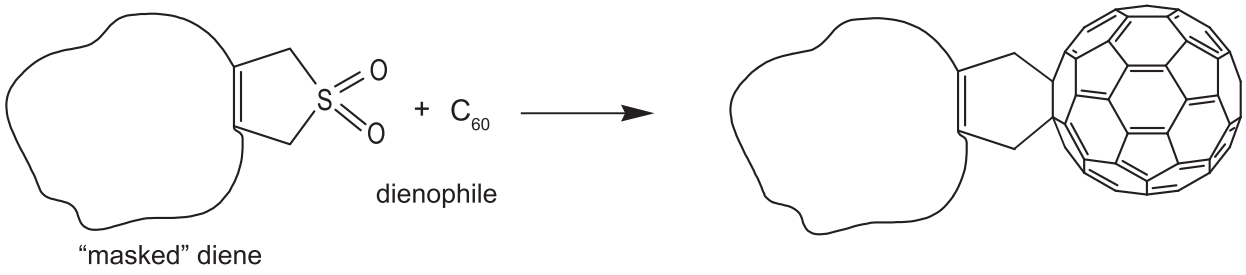

Scheme 3. Diels–Alder reaction.

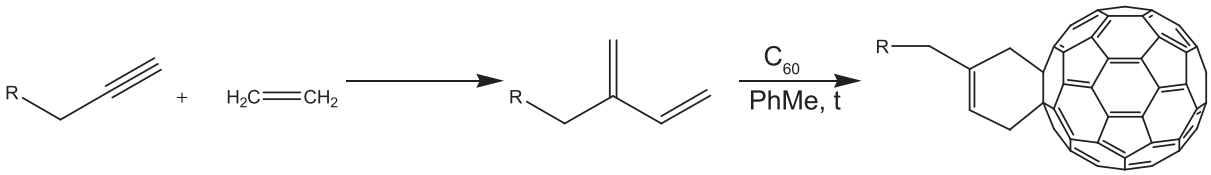

Scheme 4. Using substituted butadienes.

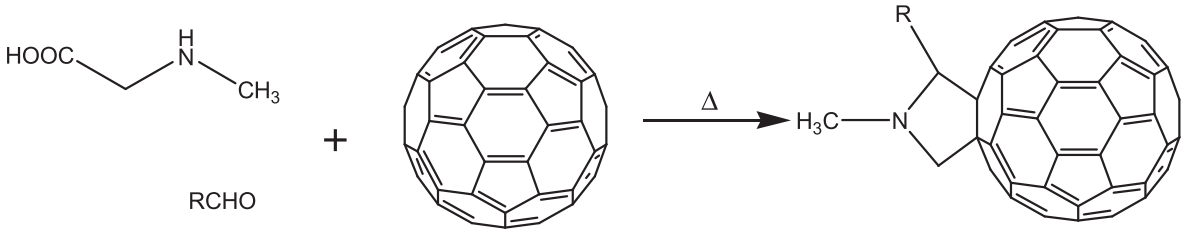

Scheme 5. Prato reaction.

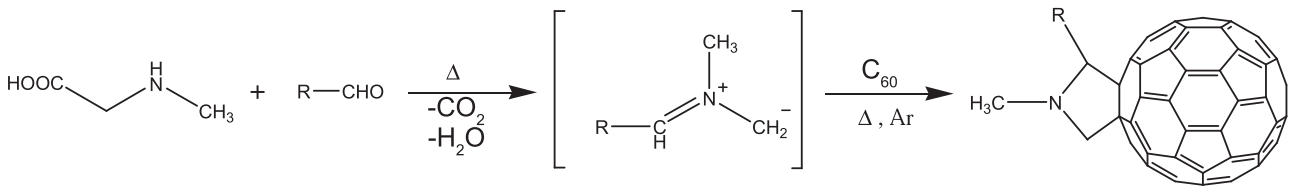

Scheme 6. The Prato reaction mechanism.

Fullerenes and, specifically, C_{60} are powerful electron acceptors and are very reactive toward electrophilic substitution. Along with the characteristic covalent σ-bonding, fullerenes are known to form rather stable conjugates held together by noncovalent forces, *i.e.* π–π stacking interactions, donor–acceptor bonds, hydrophobic inclusion interactions, and other bonding interactions with different classes of organic compounds. Among these structures, the porphyrin-fullerene complexes are of particular interest.

2. Synthesis of Covalently Linked Conjugates of C_{60} Fullerene

Granted the remarkable versatility of the synthesis strategies, there are five main methods of fullerene functionalization:

Organic azides + C_{60}. Condensation of azides with C_{60} fullerene is generally performed in hydrophobic solvents such as toluene, chlorobenzene, 1,2-dichlorobenzene, etc. and typically requires long reaction times under heating conditions (Scheme 1);

Using active methylene group of malonates (Bingel functionalization). The condensation with diethyl malonate as well as other malonic esters is effected by treatment with iodine under basic conditions (Scheme 2);

Diels–Alder Reaction with cyclic sulfones. The latter in this case act as dienophiles (Scheme 3). Unlike the two above condensations, this reaction takes place under milder conditions and affords good yields;

Condensation of C_{60} fullerene with substituted butadienes. The synthesis is based on the enyne metathesis/ Diels–Alder sequence, that is, an interaction of a terminal alkyne with olefin in the presence of Grubbs catalyst (Scheme 4) followed by the condensation of thus generated substituted butadiene with C_{60} at heating similarly to the first method;

Prato reaction. The method is based on 1,3-dipolar cycloaddition of an ylide generated by the condensation of *N*-methylglycine (sarcosine) with an aldehyde to C_{60} (Scheme 5).

This approach is widely used for the functionalization of fullerenes and in particular, in the syntheses of porphyrin-fullerenes. The reaction proceeds via the intermediate azomethine ylide which further reacts with double [6,6] bonds of C_{60} fullerene in a 1,3-dipolar cycloaddition. (Scheme 6).

The cycloaddition always occurs on the 6,6 ring position in a fullerene sphere to yield pyrrolidinofullerene. The use of other *N*-substituted glycines instead of sarcosine makes it possible to introduce two different substituents into the pyrrolidine ring. The Prato reaction has a diverse range of applications in the field of organic materials; many comprehensive reviews[2-7] and books[8-11] are available on the topic.

When run with the large excess of amino acid and aldehyde, the reaction may occur as multiadditions onto C_{60} affording fullerene with two, three, and more pyrrolidine addends.[12,13]

3. Porphyrin-Fullerene Conjugates

The conjugates of porphyrins with fullerenes (mainly with C_{60}) are of special importance among the versatile fullerene compounds. This is largely due to the high affinity between fullerene and porphyrin and their electronic complementarity. The conjugated π-system of the porphyrin macrocycle absorbs light in the wide UV-Vis-NIR spectral range, which allows using porphyrins as well as di- and tetrahydroporphyrins as light-harvesting antennas. By contrast, fullerenes show weak light absorption in the visible and near-infrared regions but are excellent electron acceptors. Based on this combination, molecular porphyrin-fullerene assemblies are employed for the construction of photosynthetic models and for the design of artificial systems that efficiently process solar energy. Porphyrin-fullerene structures are the key components of various photoelectrical devices, they find use in nanocomposites and are of high potential value in nanotechnology engineering. Their application in medicine promises far-reaching advances.

3.1. Nucleophilic Cyclopropanation of C_{60} Fullerene with Malonates

This is a rather common approach to prepare porphyrin conjugates with C_{60} that in a number of works was employed to derive fairly complex structures.[14-19] In conjugate **1**, Zn-porphyrin is rigidly bonded to two points of the C_{60} cage at two opposite positions so to provide electron transfer in the system – as anticipated by the authors (Figure 1).[14] In the second conjugate **2**, the fullerene attaches to only one point of the C_{60}.[15] Despite this difference, the photophysical and electrochemical properties of **1** and **2** are rather similar, indicative of the considerable contribution of noncovalent interactions between Zn-porphyrin and fullerene to the donor-acceptor electronic coupling which thus is not controlled by the covalent bonds.

No such resemblance was observed between *meso*, *meso*-linked [60]fullerene-oligozincporphyrin arrays **3a-c**[16] and triply-linked diporphyrin-bis[60]fullerene conjugate **4** which was shown to reversibly accommodate up to 15 electrons and possess exceptional redox and photophyscal properties.[17,18] The essential difference in the photoinduced energy-transfer and electron-transfer processes in **3a** and **4** is illustrated in Figure 2.[19]

In **3a**, photoexcitation of any subunit results in an electron transfer from the porphyrin to C_{60} with the sensitized emission in the NIR region. Photoexcitation of the C_{60} moiety in **4** results in C_{60}→porphyrin energy transfer with near-IR fluorescence of the porphyrin.

Cyclopropanation with rather complex malonate precursors (**5** in Scheme 7) was used to derive hexaadducts of C_{60} fullerene.[20] The preliminary experimental work was done to adjust the successive cyclopropanation conditions such that would afford fullerene with one or six malonate addends each terminated with two ferrocene moieties – **6** and **7**, respectively (Scheme 7).

The proved multiaddition conditions were then used to synthesize the hexasubstituted fullerene with one porphyrin unit, **10a**,**b** (Scheme 8). The starting substituted porphyrin **8** was condensed with C_{60} by the known procedure[21] to yield porphyrin–fullerene dyad **9**. The following treatment of **9** with ferrocenyl malonate **5** provides the addition of five ferrocenyl malonate molecules to the remaining octahedral double [6:6] bonds of **9** leading to symmetrical

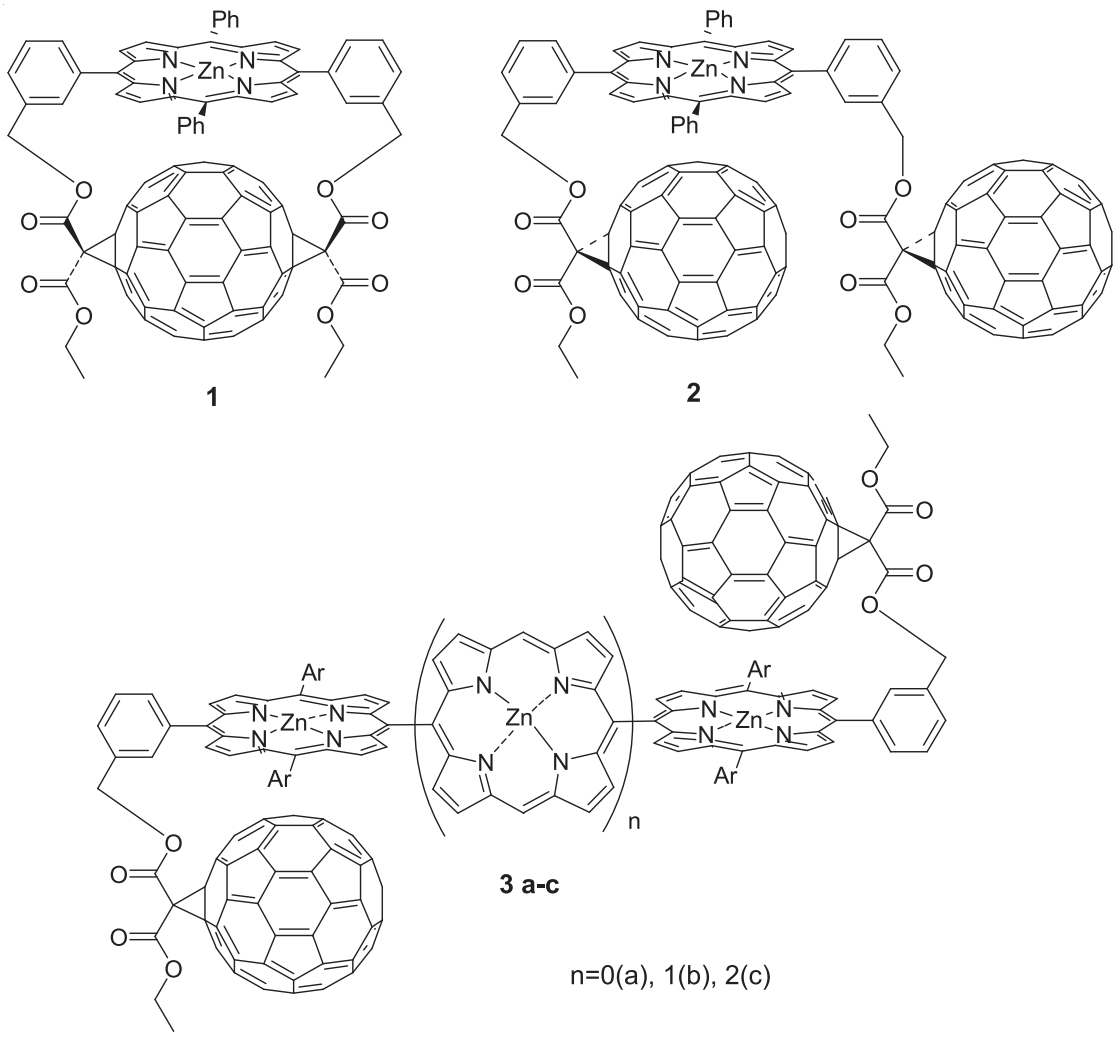

Figure 1. Porphyrin-fullerene systems based on cyclopropanated C_{60} fullerene.

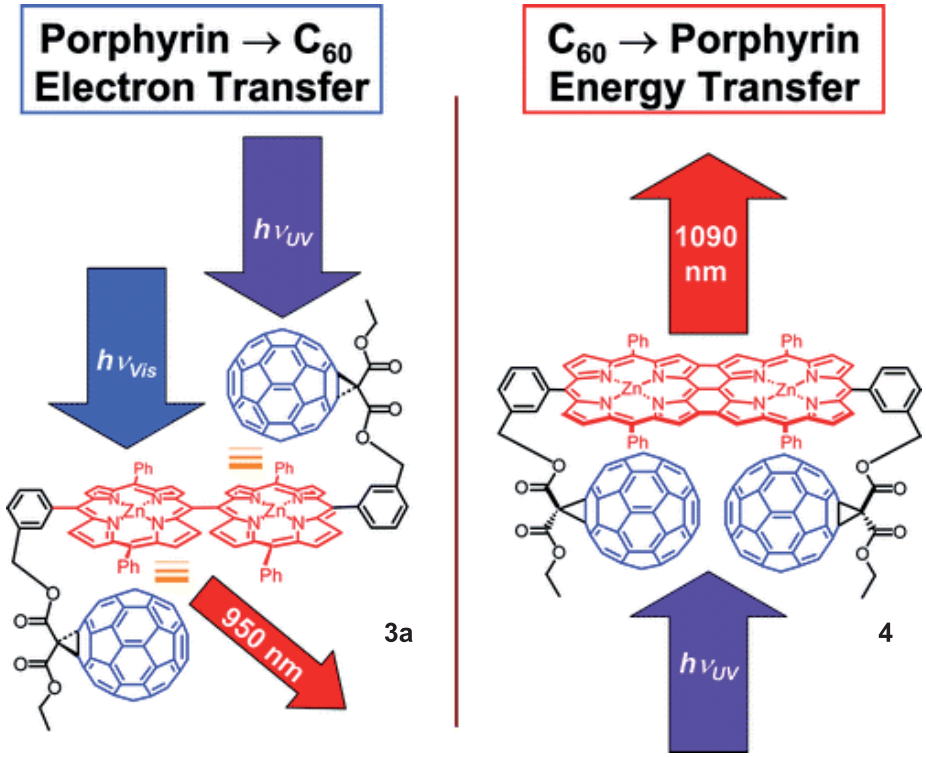

Figure 2. Photoinduced processes in structures **3a** and **4**.

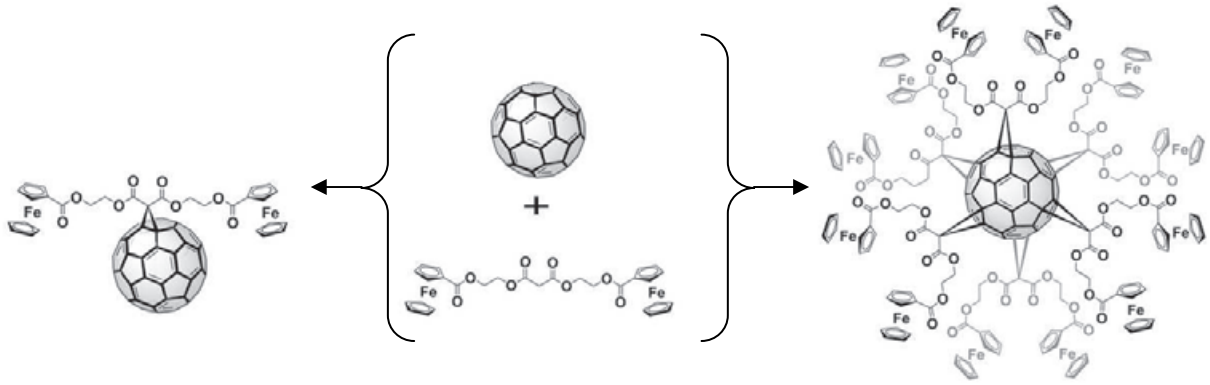

6 **5** **7**

Scheme 7. Cyclopropanation of C_{60} leading to mono- and hexasubstituted fullerene derivatives.

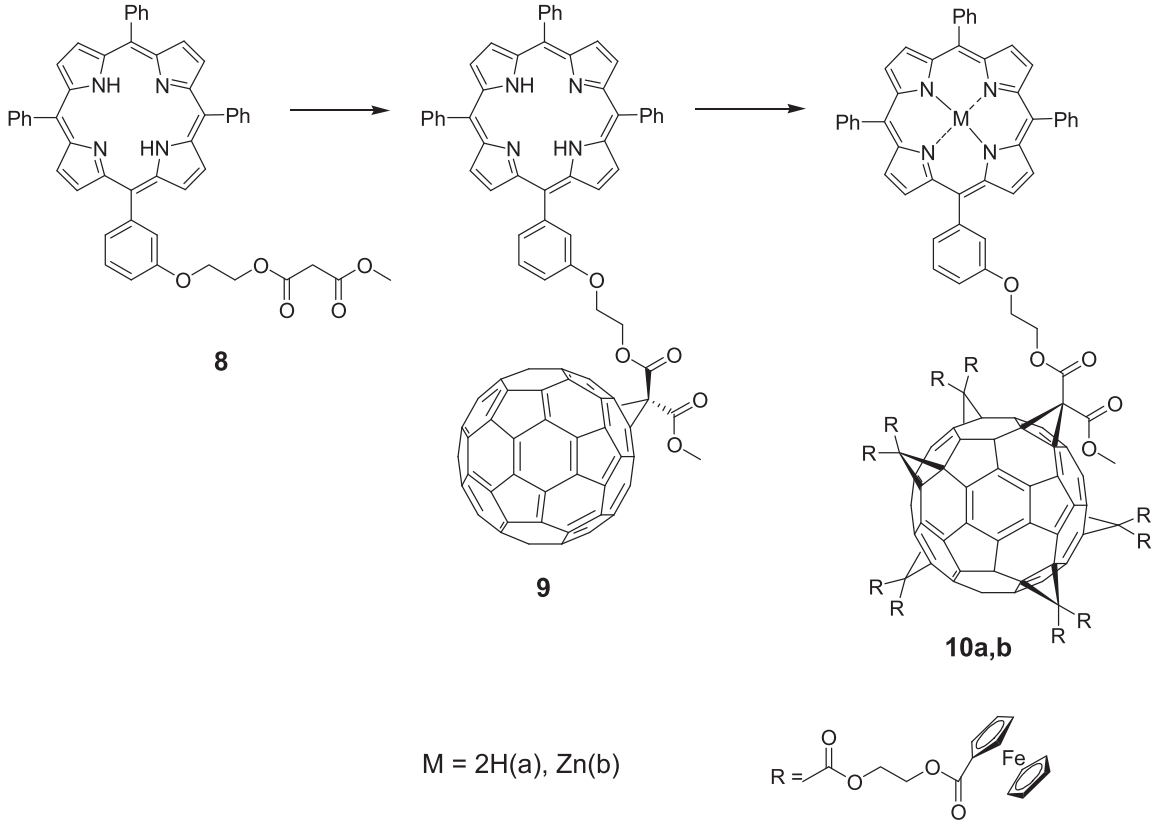

8 **9** **10a,b**

M = 2H(a), Zn(b)

Scheme 8. Synthesis of substituted C_{60} with 10 ferrocene-containing and one porphyrin addends.

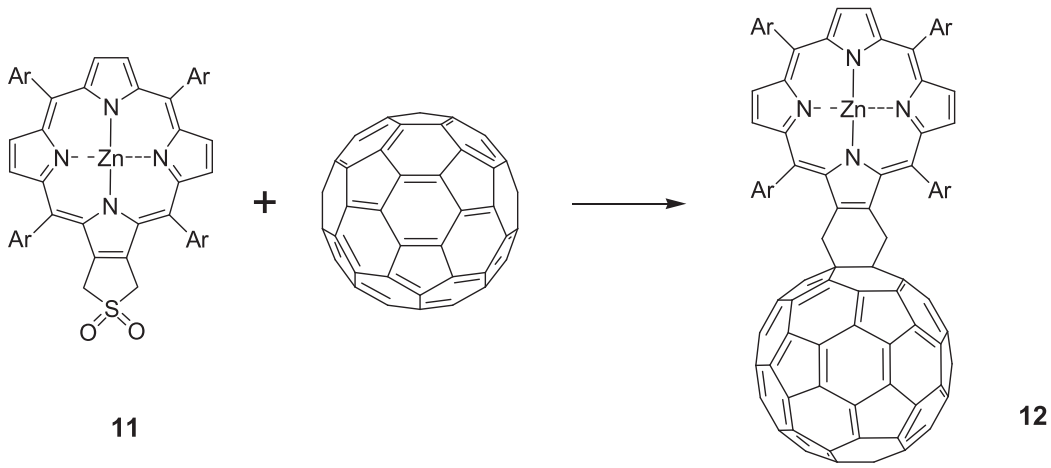

11 **12**

Scheme 9. Synthesis of porphyrin-C_{60} adducts utilizing Diels–Alder reaction.

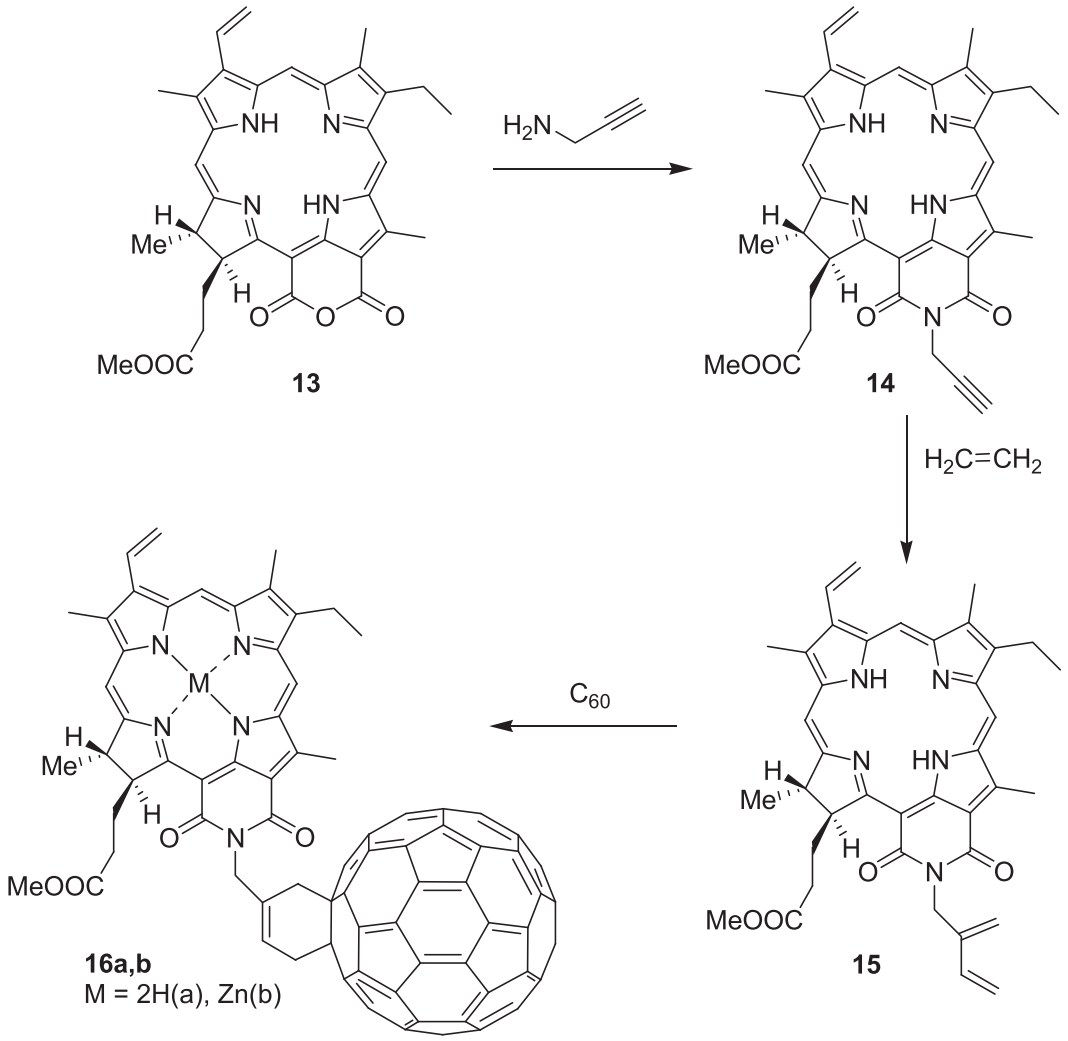

Scheme 10. Synthesis of chlorin-C_{60} conjugates.

mixed [5:1]hexakisadduct **10a** in a 30% yield and its zinc complex **10b**.

The electron withdrawing ability of C_{60} in such structures was shown to be strongly dependent on the identity of addends, which provides a means for fine tuning the energy level of the charge-separated ion-radical pair. In the monoadduct, the charge transfer from ferrocene to the singlet-excited C_{60} is an exothermic process, whereas in the hexaadduct it is always endothermic. With the appropriate solvent, the addition of the Zn-porphyrin to C_{60} already bearing five doubly ferrocenyl-functionalized addends (in all – 10 ferrocenyl groups) will result in a more exothermic electron transfer from the singlet excited state of Zn-porphyrin to hexasubstituted C_{60}. The aforesaid properties offer good platforms for using these compounds as convenient building blocks for the design and assembly of multicomponent donor-acceptor systems.

3.2. Synthesis of Porphyrin-C_{60} Adducts via Diels–Alder Reaction

An illustration of using the Diels–Alder reaction to produce porphyrin-fullerene conjugates is the interaction between sulfonated tetraaryl substituted porphyrin **11** with C_{60} fullerene affording structure **12** in good yield (Scheme 9).[22]

3.3. Using Substituted Butadienes

This approach was employed to synthesize the conjugate of C_{60} with the chlorin p_6 having an *N*-substituted imide ring fused to the macrocycle (imide derivative of purpurin).[23] The starting purpurin **13** was reacted with propargylamine in toluene at 80°C for 6 hours to give the corresponding purpurin-18-*N*-ethynylimide **14** in 80% yield (Scheme 10). The treatment of the latter with ethylene gas in the presence of the Grubbs catalyst at room temperature for 48 h afforded butadiene derivative of chlorin **15** in 40% yield. On heating with C_{60} in toluene, diene **15** gave conjugate **16a** in 30% yield. To study electron transfer, the latter was further converted to zinc complex **16b**.

In the fluorescence spectra of conjugates **16a** and **16b**, the emission intensity of the chlorin entity is considerably smaller than that of the reference parent chlorin, indicating the effective electron transfer to C_{60}.

In the porphyrin–fullerene dyad synthesized using cross metathesis,[24] the porphyrin and C_{60} are connected by the flexible linker providing an exquisite setting to study the influence of the donor–acceptor (porphyrin–fullerene) separation on the energy transfer efficiency. Synthesis of dyad **21a** and its zinc complex **21b** is illustrated in Scheme 11. The condensation of 4-hydroxybenzaldehyde with acryloyl chloride gives ester **18**

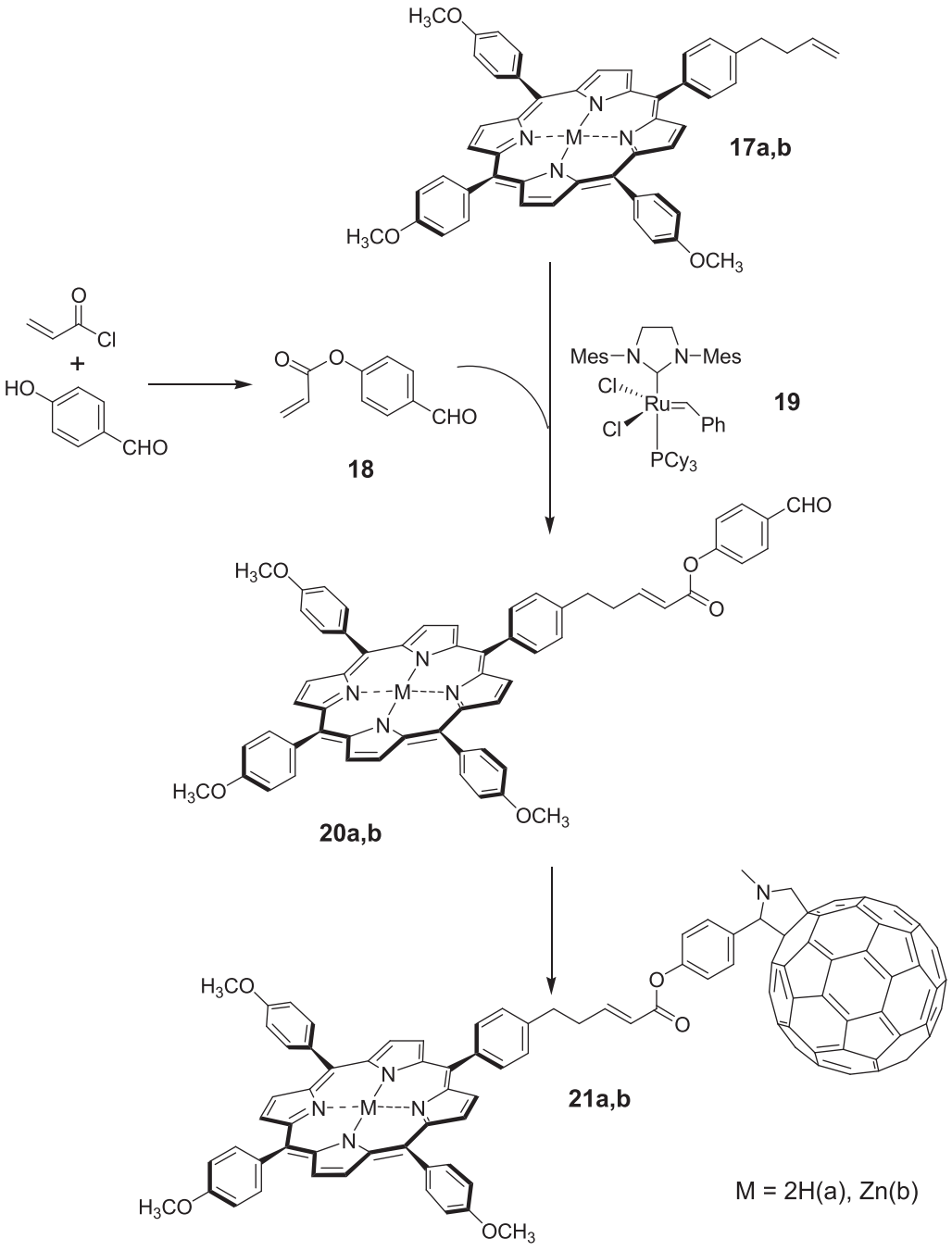

Scheme 11. Synthesis of porphyrin-fullerene dyads with flexible linkage.

in high yield. The latter reacts with porphyrin **17** in the cross metathesis in the presence of the second generation Grubbs catalyst **19** to form product **20** (yield 76%) whose formyl group affords adding C_{60} fullerene; yields of the resultant adducts **21a** and **21b** are 59 and 64%, respectively.

The photophysical characteristics of dyad **21** and, specifically, the efficiency of electron transfer and the lifetime of the charge-separated state were shown to be related to the separation distance between the porphyrin macrocycle and C_{60}.

3.4. The Prato Reaction in the Synthesis of Porphyrin-Fullerenes

There are numerous examples of employing the Prato reaction and its modifications to synthesize fullerene conjugates with porphyrins. The porphyrin and fullerene entities in these structures are connected by the pyrrole linkers, so these conjugates are actually the fulleropyrrolidinoporphyrins but are commonly referred to as fullerene-porphyrins or porphyrin-fullerenes (the latter name will be used hereafter).

All presently known porphyrin-fullerenes may be sorted into two groups. The first includes conjugates in which C_{60} and, much more rarely, other fullerenes are directly attached to the porphyrin ring either to the bound to it *meso*-aryl moieties. The structures belonging to the second group are those derived via condensing fullerenes with some compounds by the Prato reaction followed by binding with porphyrins through diverse linkers to form still more complex assemblies. Here we will only be able to touch upon the most significant and characteristic works in this field.

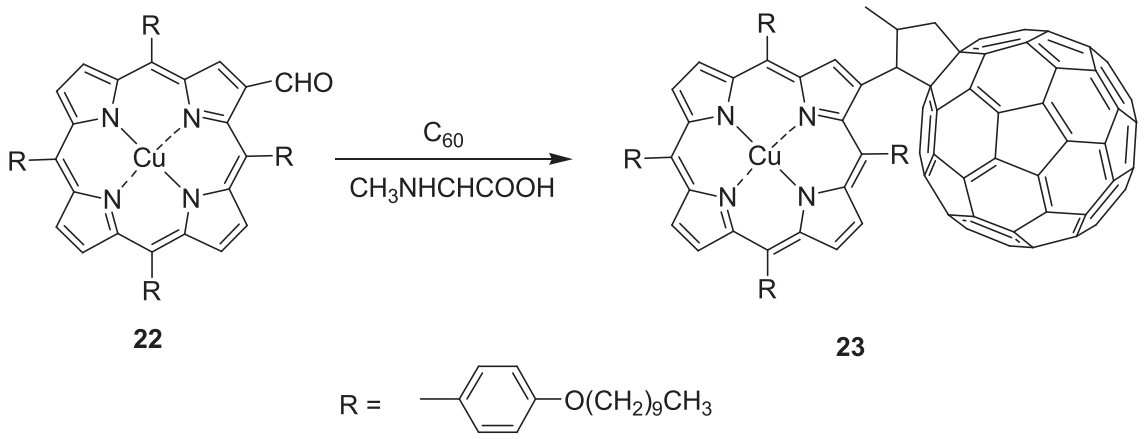

Scheme 12. Synthesis of porphyrin-fullerene complex with long-chain substituents.

The porphyrin-fullerene complex **23** has been synthesized starting from β-formyl porphyrin **22** with the four long-chain substituents (Scheme 12).[25]

Such porphyrins are typically highly soluble in organic solvents and exhibit liquid-crystalline properties.

Much more common is the Prato reaction utilizing porphyrins with formyl-functionalized *meso*-positioned aryl (typically phenyl) moieties. This strategy was used to synthesize triad **24** (a purpurin macrocycle linked to a C_{60} and to a carotenoid polyene) whose carotenoid antenna mimics the photosynthetic reaction center.[26]

In such assemblies carotenoids absorb light in the blue-green region of the spectrum at 460–540 nm (where chlorophyll has a relatively low extinction coefficient). An excitation with light absorbed by either the purpurin or C_{60} generates the initial charge separated state, C–Pur$^{\bullet+}$–$C_{60}^{\bullet-}$. The final charge separated state, C$^{\bullet+}$–Pur–$C_{60}^{\bullet-}$, is formed in one of the compounds with a quantum yield of 32% based upon light absorbed by the polyene antenna.

The synthesis and photophysical properties of the artificial photosynthetic reaction center (Scheme 13, structure **29**) composed of the two porphyrins performing as electron donors rigidly linked to C_{60} fullerene acting as electron acceptor are reported.[27] The two porphyrins are closely spaced, in an arrangement reminiscent of that of the special pair in bacterial reaction centers. Electron transfer from the excited porphyrin yields P$^{\bullet+}$– $C_{60}^{\bullet-}$ ion-radical pair with a lifetime of 1.1 ps. The first step (not shown in Scheme 13) of the synthesis procedure was the Pd-catalyzed condensation of the porphyrin containing *meso*-(4-iodophenyl) group with phenylacetylene-substituted porphyrin leading to dimer **25**. The latter was condensed with the substituted furan **26** by the Diels–Alder reaction (Scheme 13). The removal of carbon monoxide and introduction of Zn yielded dyad **27**. The ester group in dimer **27** was reduced with $LiAlH_4$ to the alcohol, the oxidation of the latter with MnO_2 afforded aldehyde **28**. The following double Prato reaction furnished triad **29** in a 20% yield.

The intermediate ylides in the Prato reaction may be synthesized starting with *N*-substituted glycines different from sarcosine to afford a variety of functionalized fullerenes or porphyrin-fullerenes. Thus, a glycyl-substituted porphyrin **31** was utilized as a starting compound for the synthesis of a π–π-stacked porphyrin–fullerene dyad with a frozen geometry.[28] An ester **31a** was synthesized via the condensation of initial 5-(2-aminophenyl)-10,15,20-triphenylporphyrin **30** with methyl iodoacetate (Scheme 14).

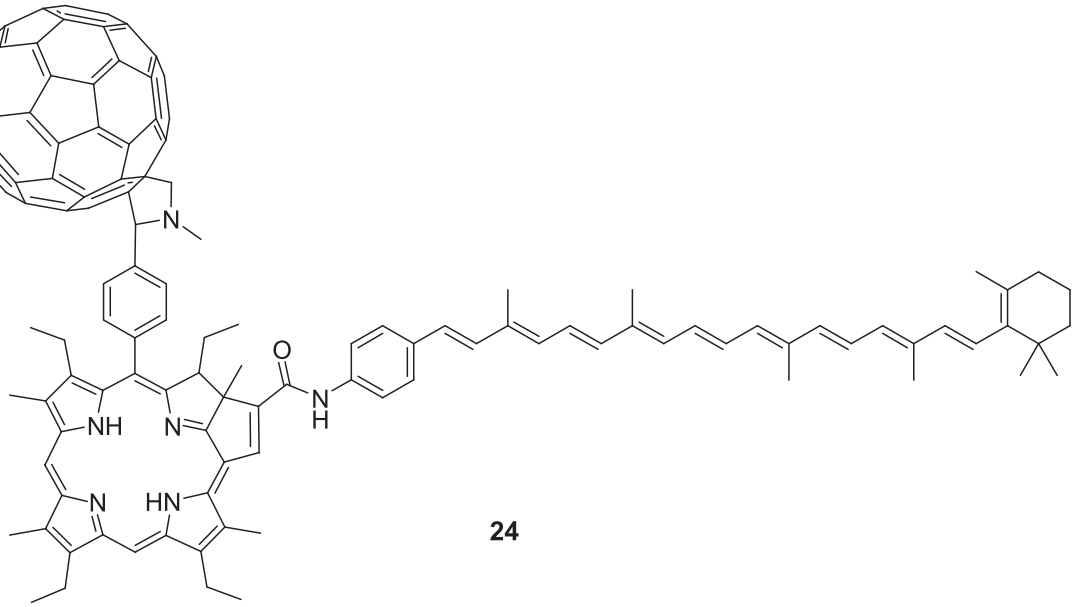

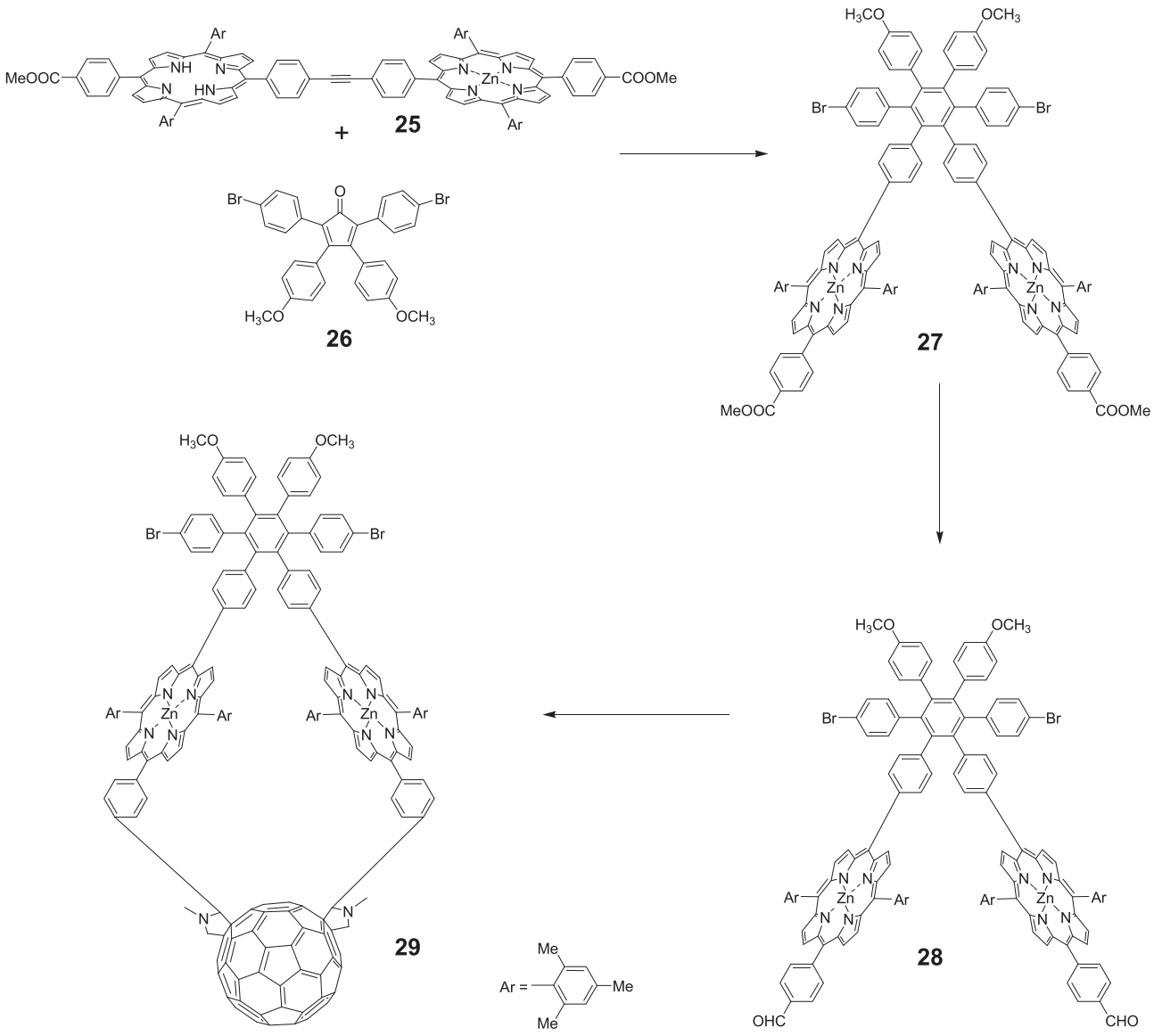

Scheme 13. Synthesis of diporphyrin-fullerene assembly.

The following saponification gave the acid **31b**, which was heated with benzaldehyde and C_{60} to afford dyad **32**.

The NMR revealed a strong interaction between the two chromophores, enabled by their short separation due to the constrained geometry forcing the fullerene molecule to lie on the porphyrin plane.

The successful strategy has been developed to prepare photoconductive visible-light-excited nanostructures based on chiral dyad **33**.[29] The dyad was synthesized via azide-alkyne click [3+2] cycloaddition between porphyrin bearing the *meso*-phenyl ring bound azide and alkyne-functionalized C_{60} fullerene.

Dyad **33** self-assembles into nanofibers with an exceptionally high charge-carrier mobility making these macromolecules of potential utility for photovoltaics.

Electroconductive structures **34-36** were prepared by assembling the fulleropyrrolidine synthesized by the Prato reaction with the Zn-porphyrin using the substituted [2,2']-paracyclophanes as spacers with lengths controlled by the size of oligo(phenylene vinylene) chain.[30]

In accordance with the Marcus theory, the coupling between electron donor and electron acceptor depends on the separation distance between them as well as the identity of the spacer connecting the donor and acceptor entities, especially on its electronic properties. The charge recombination rate constants observed for the donor–acceptor dyads with C_{60} are markedly higher compared to the relevant dyads with quinones.

There are a large number of reports on using the Prato reaction to synthesize porphyrin–fullerene dyads with a variety of spacers. One of the recent examples is the synthesis of the Zn-porphyrin–C_{60} dyad with the diphenylsilane bridge **37**.[31] Such structures as well as the more complex oligo- and polysilanes exhibit a unique σ-conjugation, that is, delocalization of σ-electrons over the silicon backbone. Importantly, σ-delocalization is strongly dependent on the chain backbone configuration. The aforesaid work studies the effect of the conformation on electron transfer.

The remarkably complex porphyrin–fullerene arrays were prepared through the Prato reaction with a C_{60} fullerene

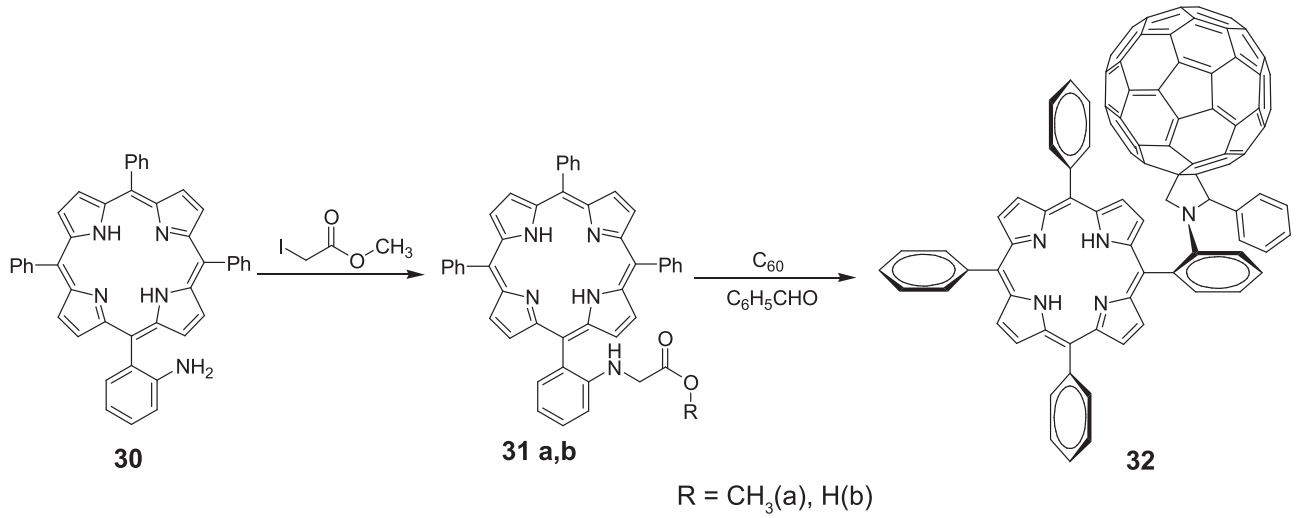

Scheme 14. The Prato reaction with glycyl-substituted porphyrin.

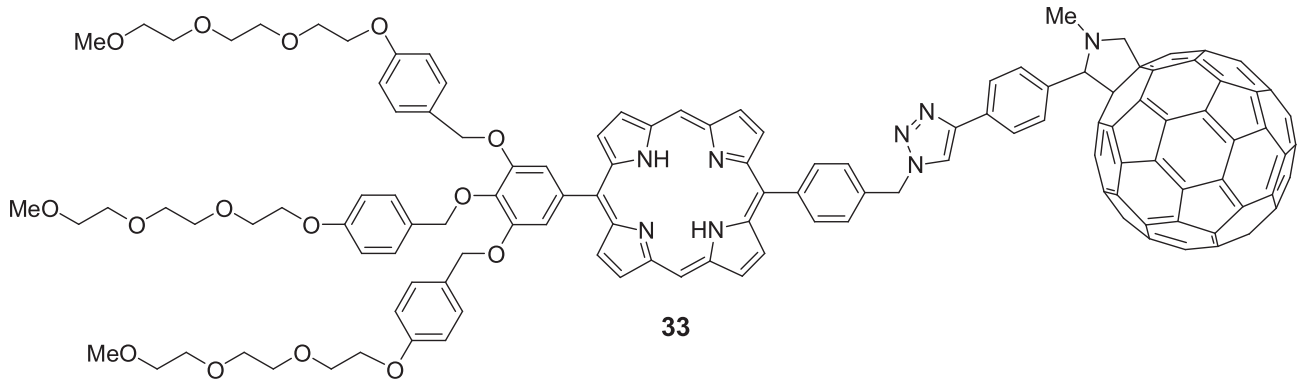

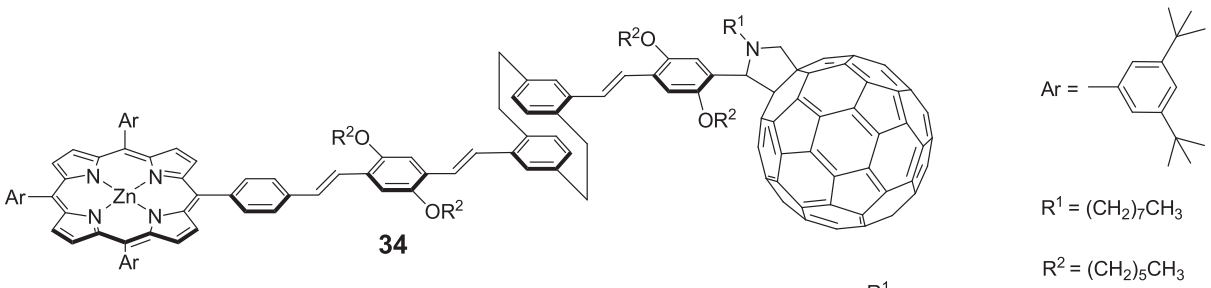

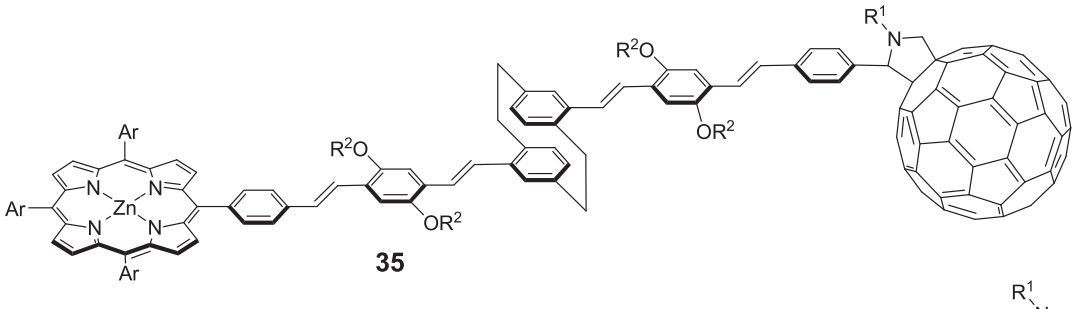

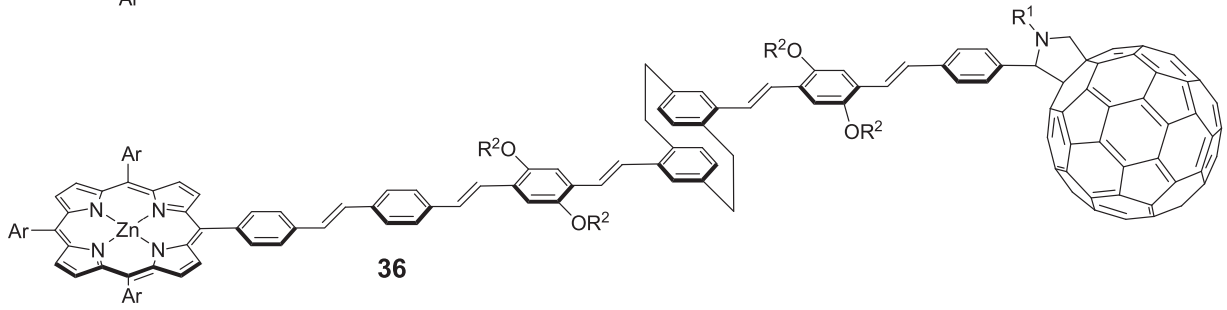

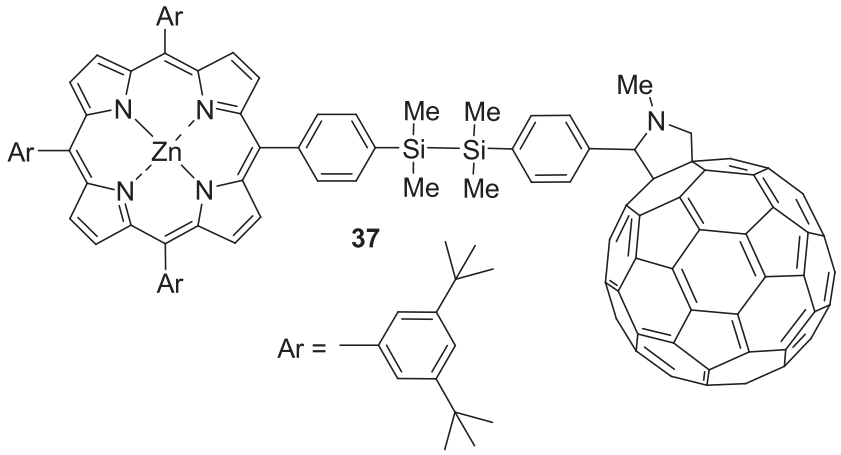

derivative bearing a benzaldehyde moiety.[32] Scheme 15 shows the condensation of such building block **38** with pyrrole (conducted using the Lindsey procedure for the synthesis of sterically hindered porphyrins).[33] The resulting porphyrin appended with four symmetrical C_{60} units **39** was obtained in 12% yield.

In the photophysical study, conjugate **39** was shown to produce a short-lived charge separated state. To prolong its lifetime, the authors synthesized the multiporphyrin array to be used as electron donor. The porphyrin dyad of a multiporphyrin array creates the longer path for the photoinduced electron transfer to C_{60} with a longer donor–acceptor distance that is expected to favor the formation of long-lived radical-ion pairs.[34]

The initial benzaldehyde-terminated porphyrin–fullerene dyad **40a** was condensed with pyrrole under Lindsey conditions (Scheme 16) to give assembly **41a** in a 57% yield that is relatively high for this type of structures. The molecular formula of the zinc complex **41b** ($C_{740}H_{612}N_{20}O_{48}Zn_5$) was confirmed by mass spectrometry, and the structure was assigned on the basis of variable temperature ^{1}H NMR spectra. Unfortunately, no data on the energy transfer in these structures have been reported.

However, along with the long lifetime of the charge-separated state (CS), it is desirable for artificial reaction center mimics to minimize the energy losses during electron transfer from the donor to the acceptor. The multi-step electron transfer systems, while providing the long-lived CS, result in considerable losses of energy. The solution to the problem may be in the design of well-arranged dyad and triad architectures with a short electron transport chain and the well-balanced electronic coupling between each component.

One of the examples of direct bonding of C_{60} to the porphyrinoid macrocycle is the condensation of 3-formyl-3-devinylpurpurin-18-*N*-hexylimide methyl ester **42** with sarcosine and C_{60} (Scheme 17).[35] Thus produced zinc chlorin–fullerene dyad **43** with extremely short donor–

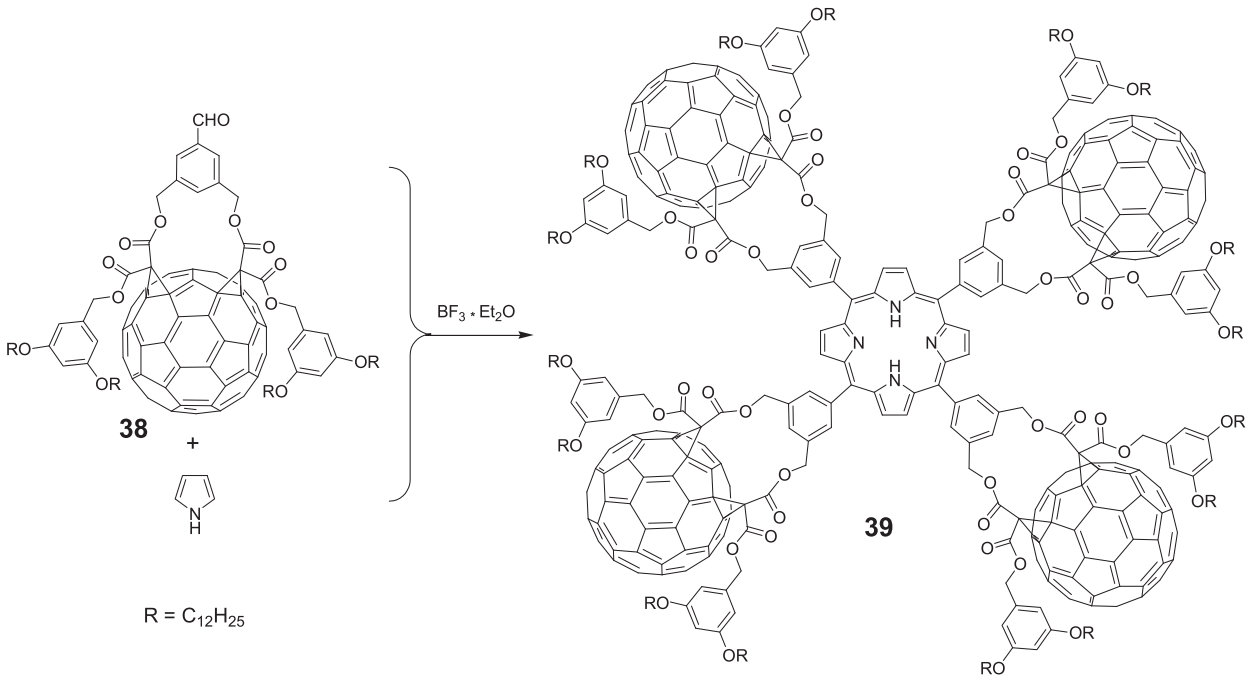

Scheme 15. Synthesis of tetraphenylporphyrin with four fullerene substituents.

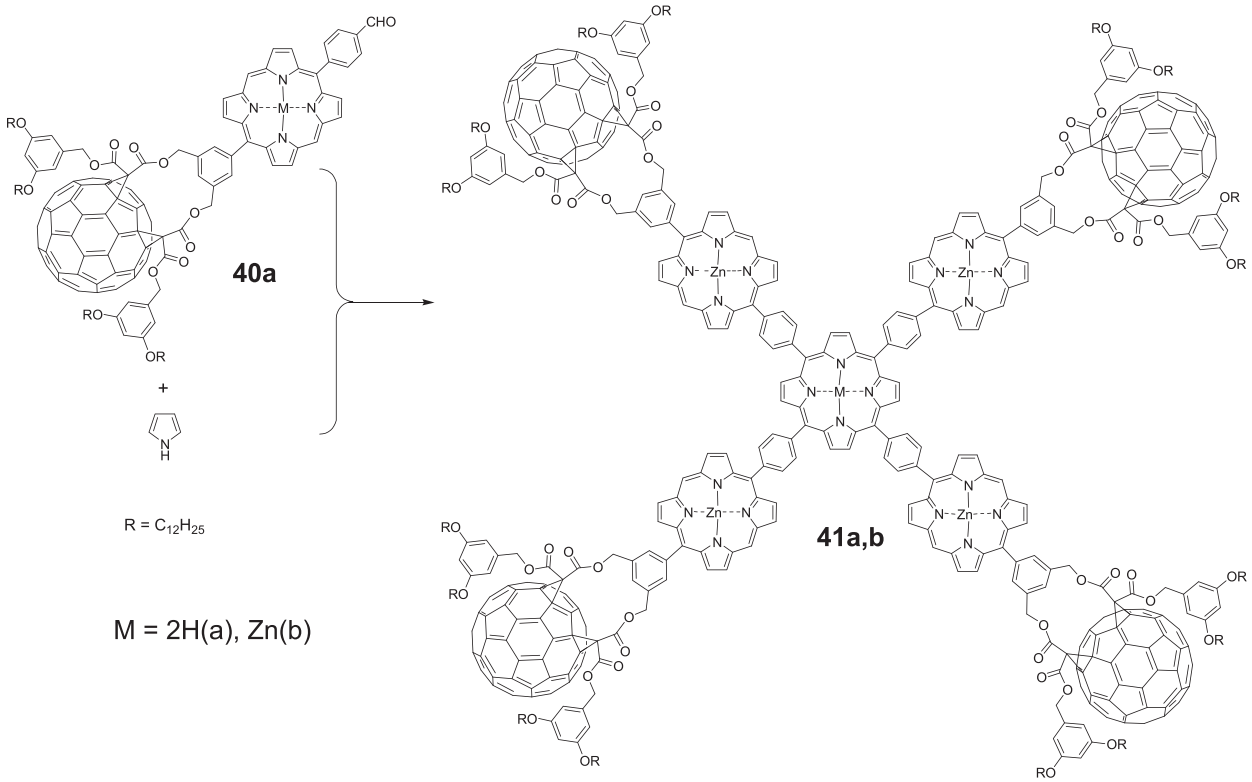

Scheme 16. Synthesis of multiporphyrin cluster with four fullerene units.

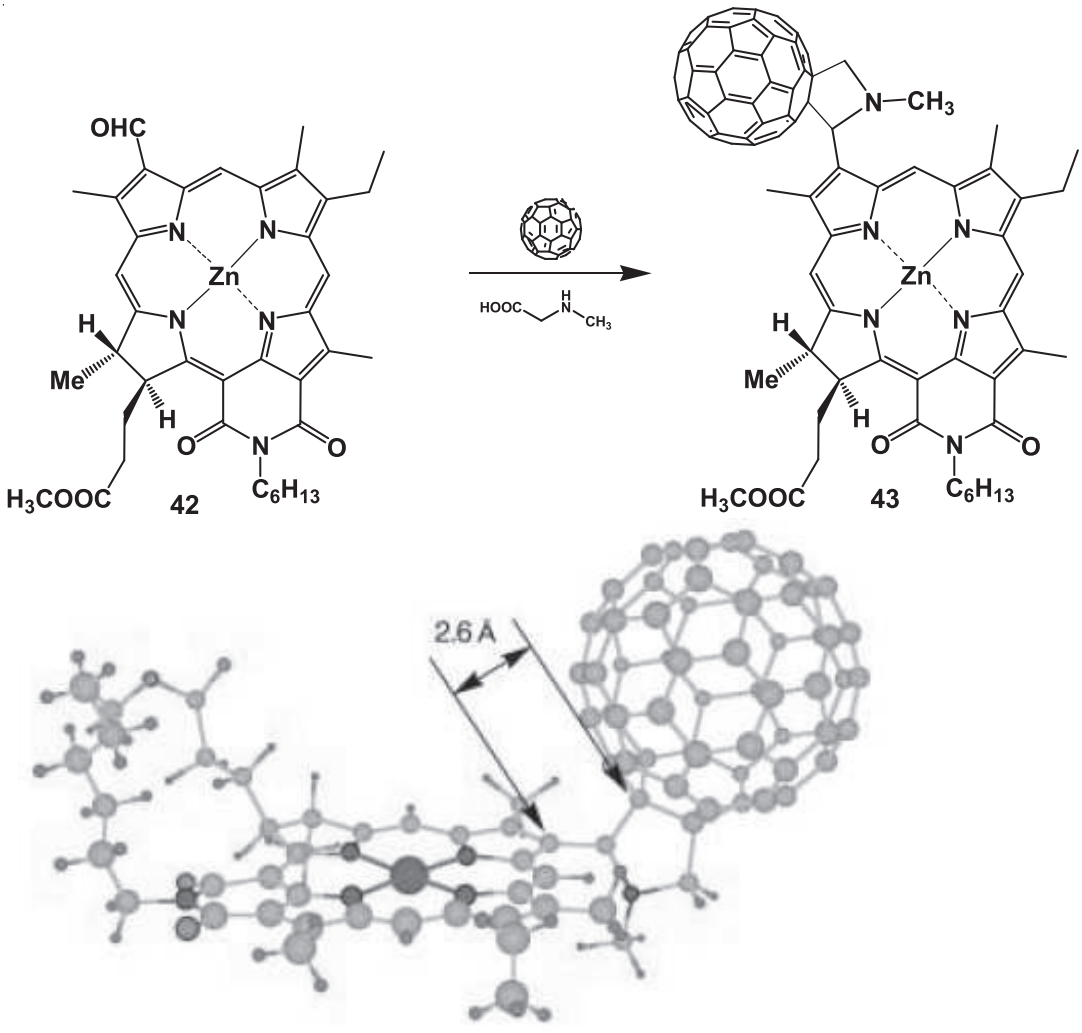

Scheme 17. Synthesis and MP3 optimized geometry of chlorin-fullerene dyad.

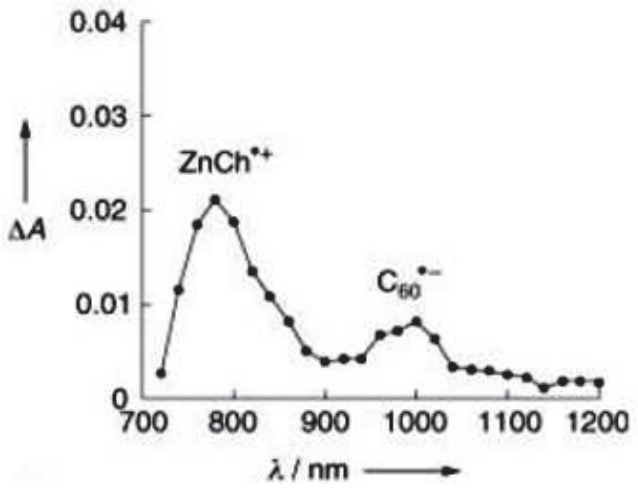

Figure 3. Transient absorption spectrum of ZnCh-C_{60} at 25° C recorded 1 μs after excitation with a 355-nm laser.

acceptor distance generates the ultra-long-lived charge-separated state Zn–Chl$^{\bullet+}$–$C_{60}^{\bullet-}$ with a rather high quantum yield (the lifetime is 230 ms at 25° C and 120 s (!) at -150° C, the quantum yield of the CS state was determined as 12%[36]). The absorption spectrum of dyad **43** (excitation with a 355-nm laser) is shown in Figure 3.

Interestingly, even a slightly less close contact between C_{60} and the chlorin macrocycle in dyad **44** results in the shortening of the lifetime of the CS state to 110 ms (at 25°C).

4. Structures with Noncovalently Linked Porphyrins and Fullerenes

The porphyrin-fullerene complexes may be held together by noncovalent interactions, in particular, coordination bonding of metalloporphyrins with strong electron-donating substituents (predominantly pyridine) and a π–π stacking between the flat aromatic system of the

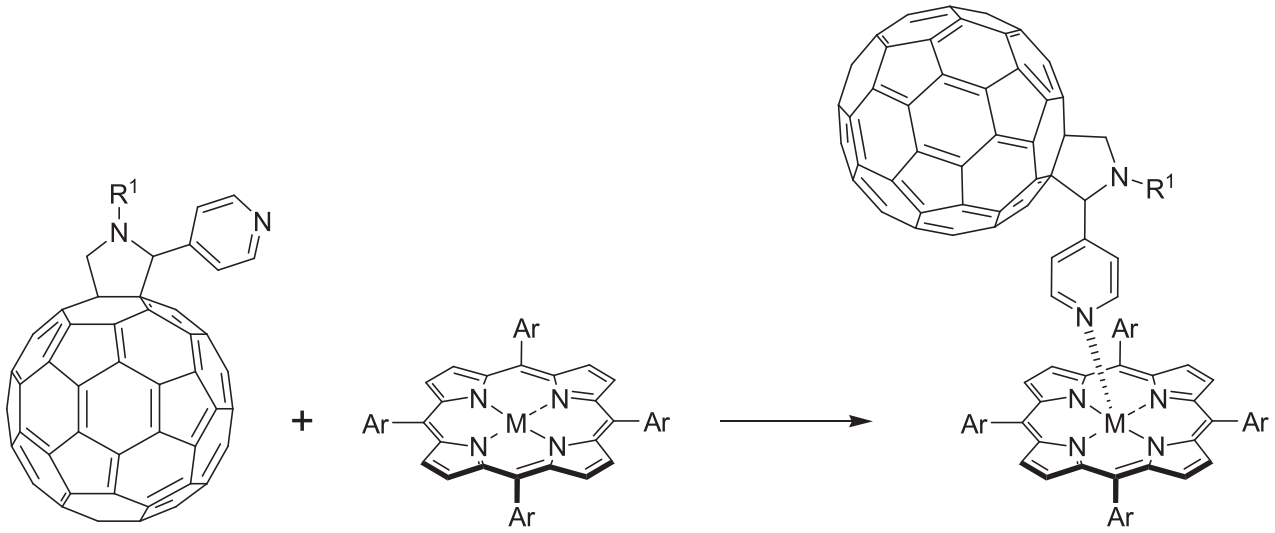

R^1 = Me(a), Triethylene glycol monomethyl ether (b)

Scheme 18. Noncovalently linked metalloporphyrin–fullerene dyads assembled via axial coordination.

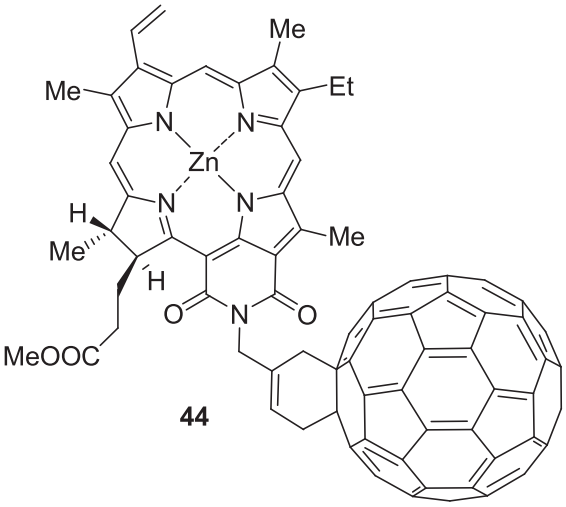

porphyrin and C_{60}. These noncovalent interactions taken individually are weak, but when several are used together, very stable molecular ensembles may result. Some structures involve the combination of the covalent linkage between porphyrin and fullerene with the noncovalent bonding of above-mentioned type.

The coordination of the metal of the porphyrin metallocomplex to the pyridyl nitrogen of fulleropyridine is a simple and effective approach to link porphyrins and fullerenes. The strategy is exemplified by the synthesis of the donor–acceptor dyads **47** and **48** (Scheme 18).[37] The strength of such complexes depends on the identity of the metal in the porphyrin macrocycle. In the zinc tetraphenylporphyrin **47**, the coordination with pyridine is weak since the only σ-bonding is present, while in the case of ruthenium tetraphenylporphyrin **48** σ-bonding is reinforced by π-backbonding.

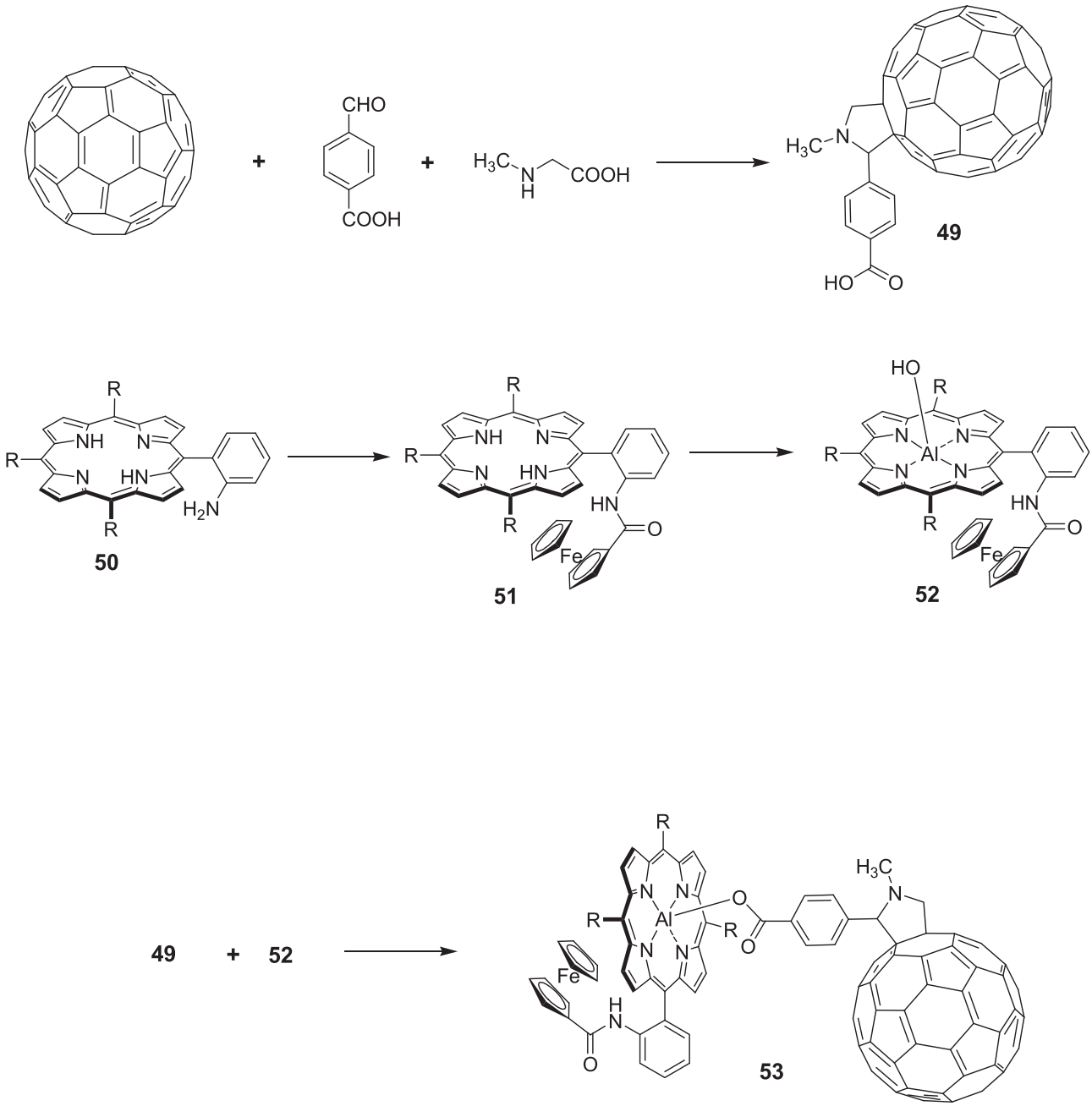

Scheme 19. Synthesis of ferrocene-Al^{III}-C_{60} porphyrin triad.

The photoinduced electron transfer rate constant for dyad **47a** was 8.6 μs in CH_2Cl_2 and up to 600 μs in polar solvents such as benzonitrile.

The linkage between the fullerene and porphyrin entities in the conjugates may involve ionic bonds. In ferrocene–Al-porphyrin–C_{60} triad (Fc–AlPor–C_{60}) **53**, the fullerene unit is bound axially to the aluminum(III) porphyrin via a benzoate spacer.[38] The triad was synthesized in three steps. The Prato reaction was employed to condense C_{60} with *n*-carboxybenzaldehyde and *N*-methylglycine into substituted fulleropyrrolidine **49** (Scheme 19). Acylation of the terminal amino group of porphyrin **50** with the ferrocenecarboxylic acid yielded intermediate **51** which was further converted to aluminum complex **52**. The following addition of **49** to **52** afforded rather stable triad **53**. In the triad, excitation of the porphyrin gives rise to the charge-separated state $Fc^{\bullet+}$–AlPor–$C_{60}^{\bullet-}$ in two electron transfer steps.

A trimer **56** with the porphyrin macrocycles connected through flexible spacers, and its noncovalent conjugate with C_{60} **57** (Scheme 20) were synthesized in an attempt to generate long-lived charge-separated states mimicking natural photosynthetic processes and the photoconversion in special pairs (the characterization of photoinduced electron transfer from the porphyrin array to fullerene is given in detail).[39] Structure **56** was afforded by azide-alkyne click cycloaddition between azide-bearing Zn porphyrin **54** and tripropargylamine **55** in the presence of $CuSO_4 \cdot 5H_2O$ and sodium ascorbate. The porphyrin trimer was shown to be capable of the inclusion complexation with pyridyl-functionalized fulleropyrrolidine **57**, yielding complex **58** stabilized by π–π-interactions of two porphyrin macrocycles with the fullerene sphere and by the (pyridyl) nitrogen–zinc coordination (association constant is $1.1 \cdot 10^5\,M^{-1}$).

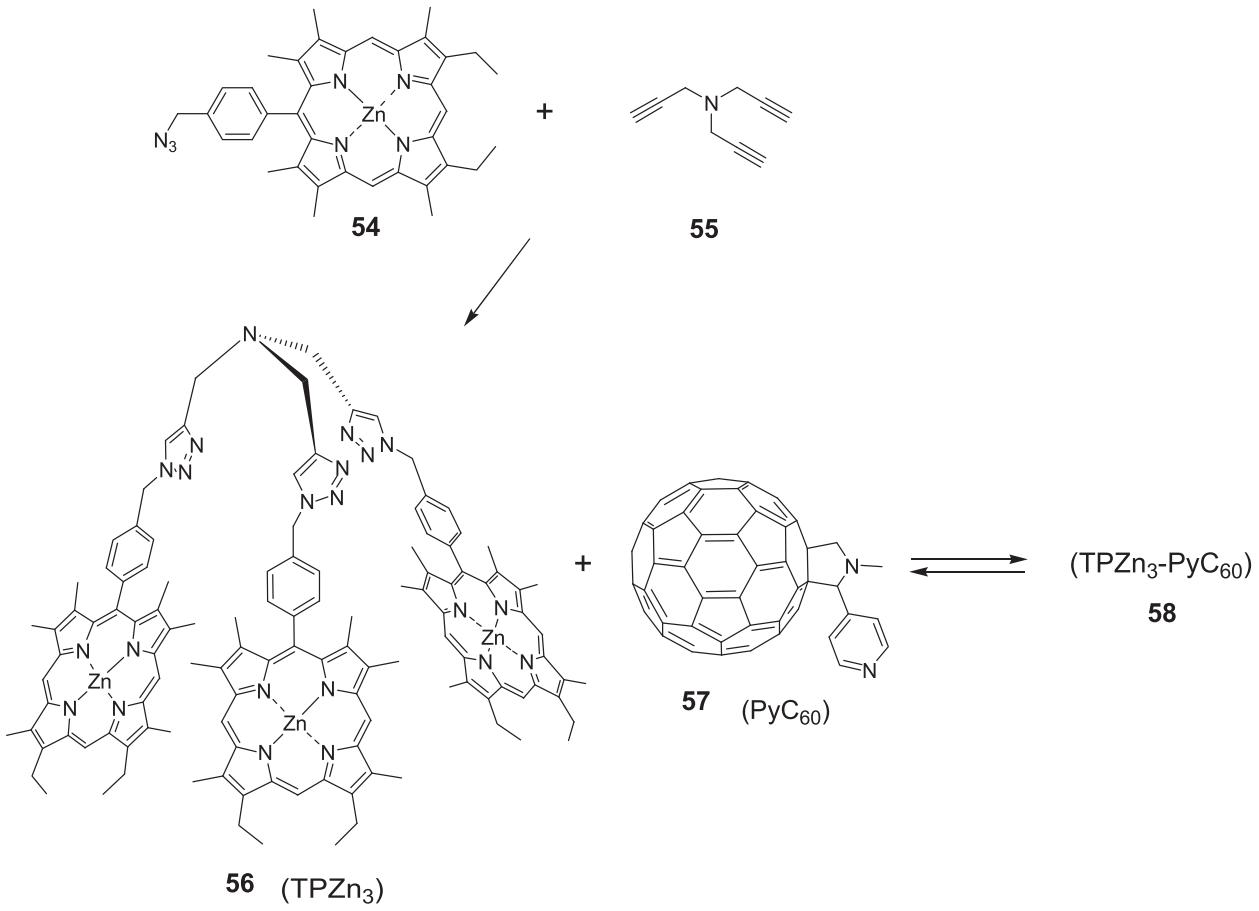

Scheme 20. Synthesis of porphyrin-fullerene structures stabilized by π–π-interactions.

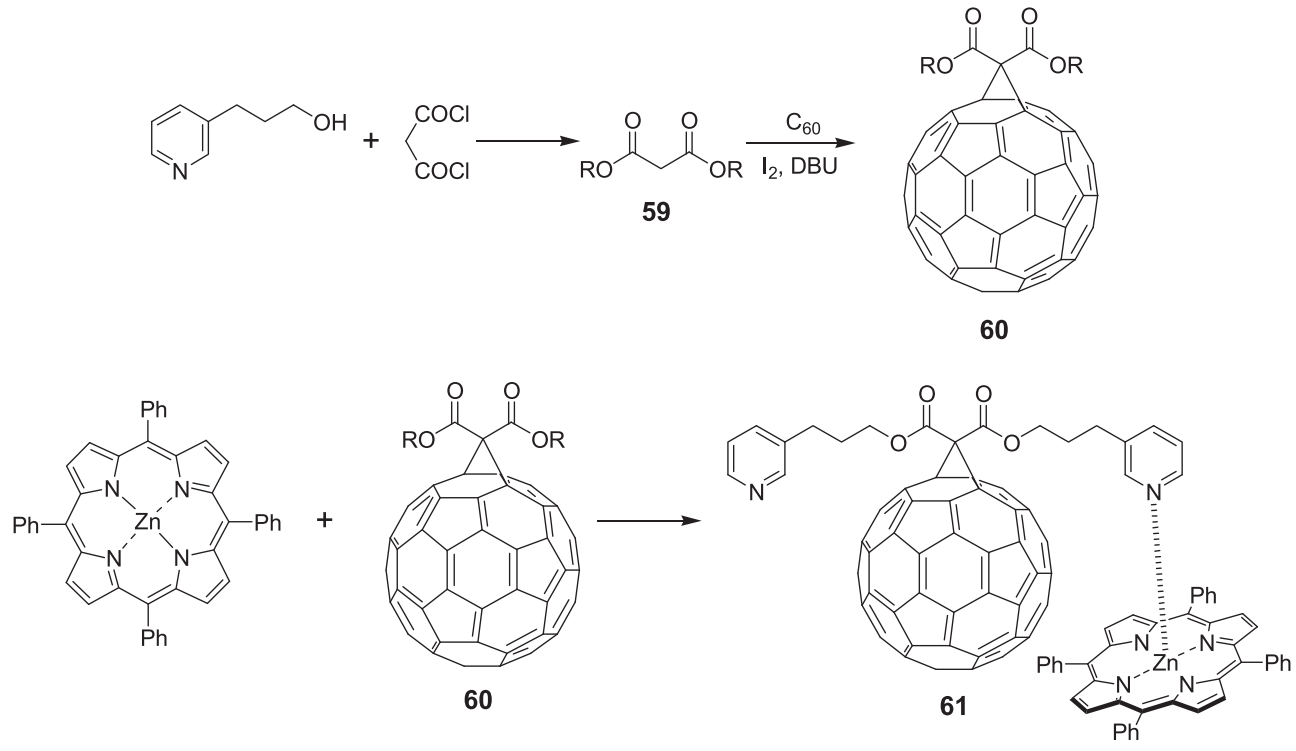

Scheme 21. Synthesis of two-point bound porphyrin-fullerene dyad.

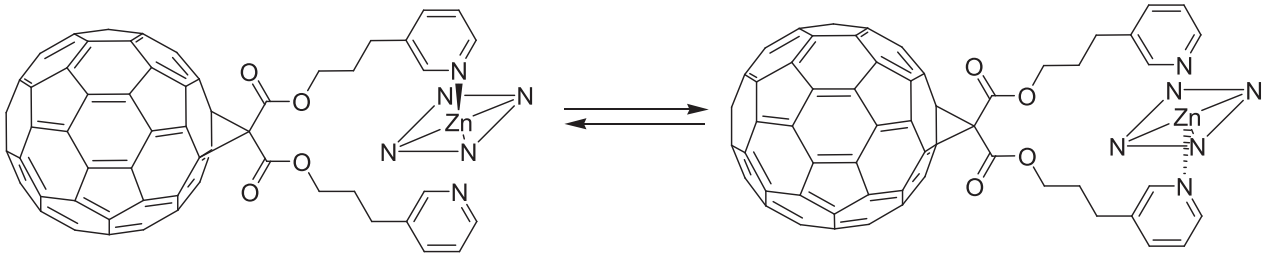

Figure 4. Dynamic process for the two-point binding of Zn-porphyrin in dyad **61**.

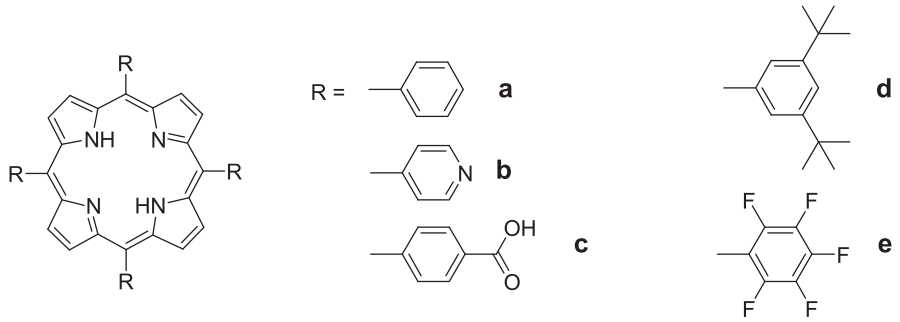

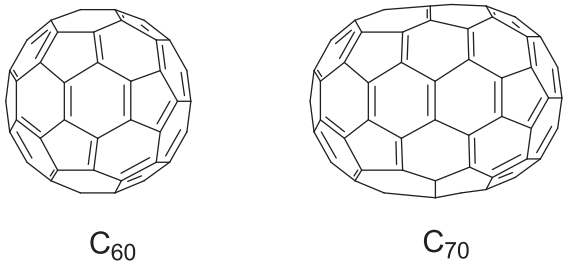

The dynamic equilibrium of the two-point binding mode involving coordination of two pyridine units to zinc in Zn-porphyrin–fullerene complex **61** is shown in Figure 4.[40] C_{60} fullerene was functionalized via cyclopropanation to **60** with di[3-(3-pyridyl)propyl]malonate **59** (Scheme 21).

Self-assembled dyad **61** derived from fullerene **60** and zinc tetraphenylporphyrin (1:1) was shown to exist in two isomeric forms in dynamic equilibrium (Figure 4).

Noncovalent binding between fullerenes C_{60} and C_{70} and protonated porphyrins in the gas phase was studied with the *meso*-substituted porphyrins **62a**–**e**.[41] The protonated complexes were generated by electrospray ionization of the porphyrin-fullerene mixture in 3:1 CH_2Cl_2:MeOH containing formic acid. All singly protonated porphyrins formed with C_{60} and C_{70} the 1:1 complexes, whereas doubly protonated porphyrins yielded no complexes.

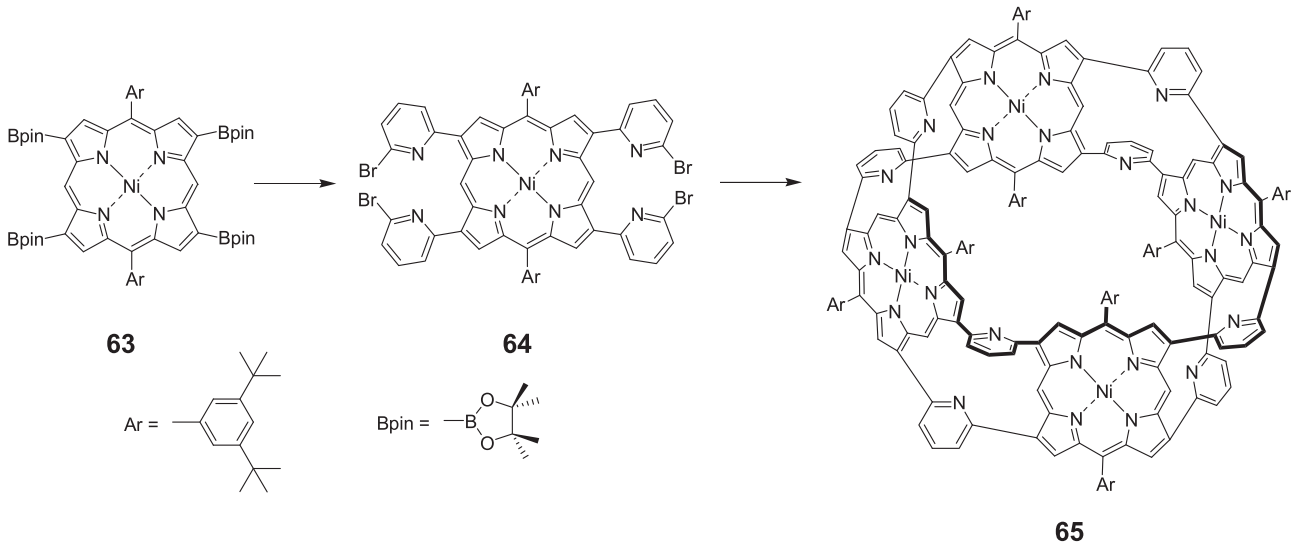

Scheme 22. Synthesis of porphyrin nanobarrel.

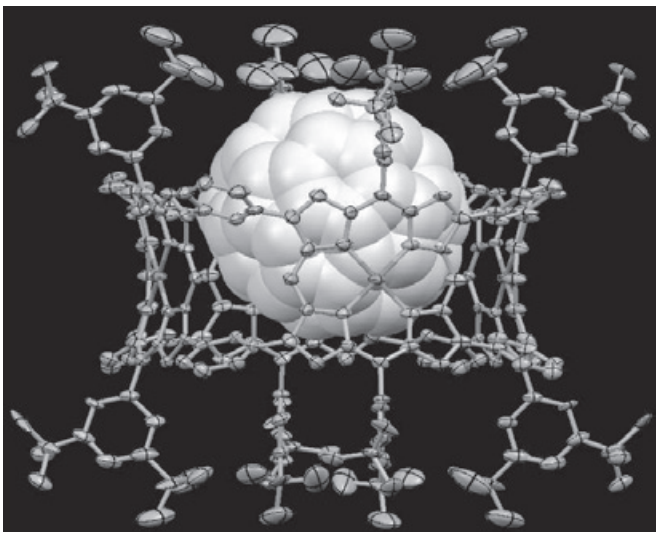

Figure 5. C_{60} encapsulated in cyclic porphyrin tetramer.

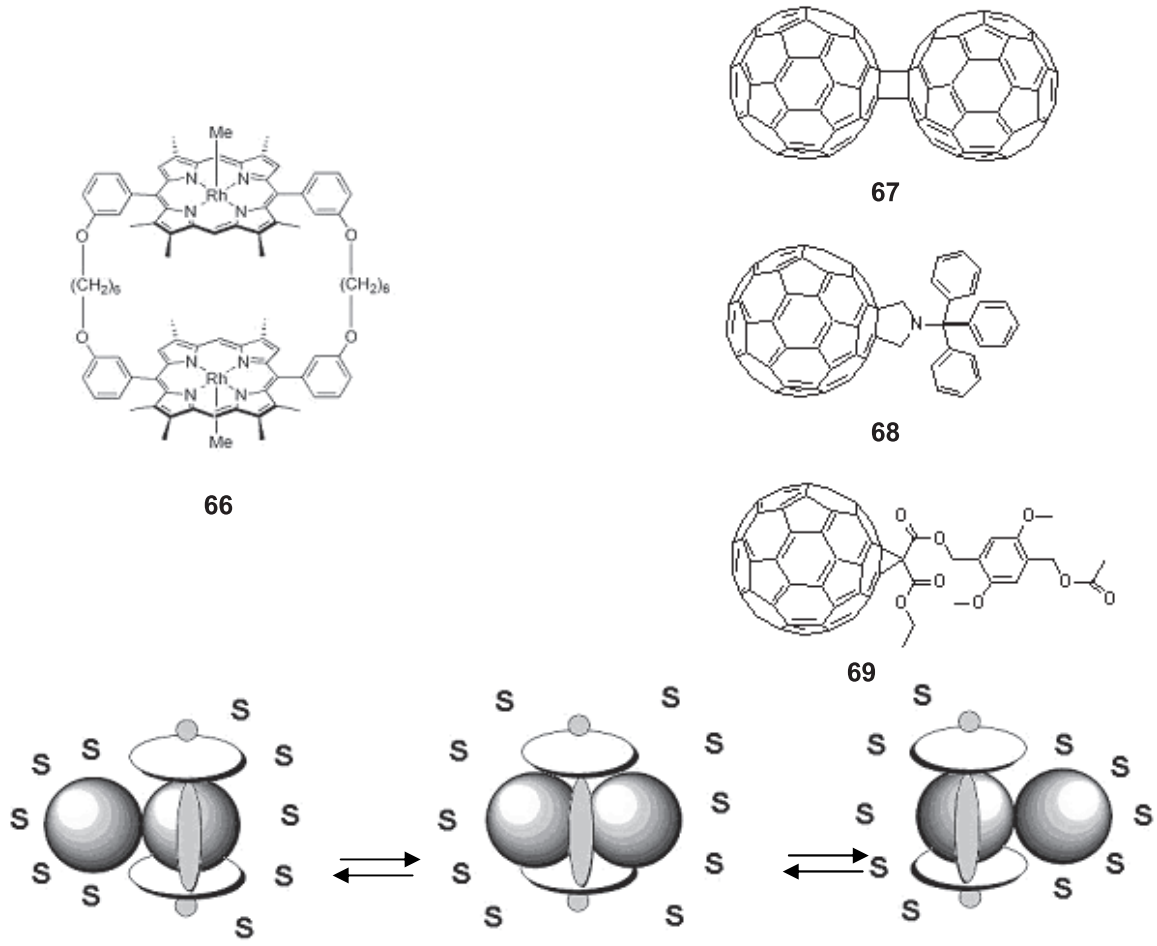

Figure 6. Supramolecular porphyrin-fullerene oscillator.

Experimental results demonstrate that C_{70} binds to the protonated porphyrins more strongly than C_{60}, and electron-donating substituents at the *meso* positions increase the fullerene binding energy, whereas electron-withdrawing substituents decrease it. Porphyrins carrying bulky substituents prefer the end-on binding of C_{70} due to the steric hindrance, otherwise the side-on binding of C_{70} is favored.

An example of the host-guest porphyrin-fullerene structure assembled via hydrophobic interactions is provided in Ref.[42] which reports the synthesis of a porphyrin nanobarrel that encapsulates C_{60}. The nanobarrel is composed of four 5,15-di-*meso* arylated porphyrin units and has a diameter of 14 Å which matches the C_{60} size fairly well. The structure of the nanobarrel with encapsulated C_{60}

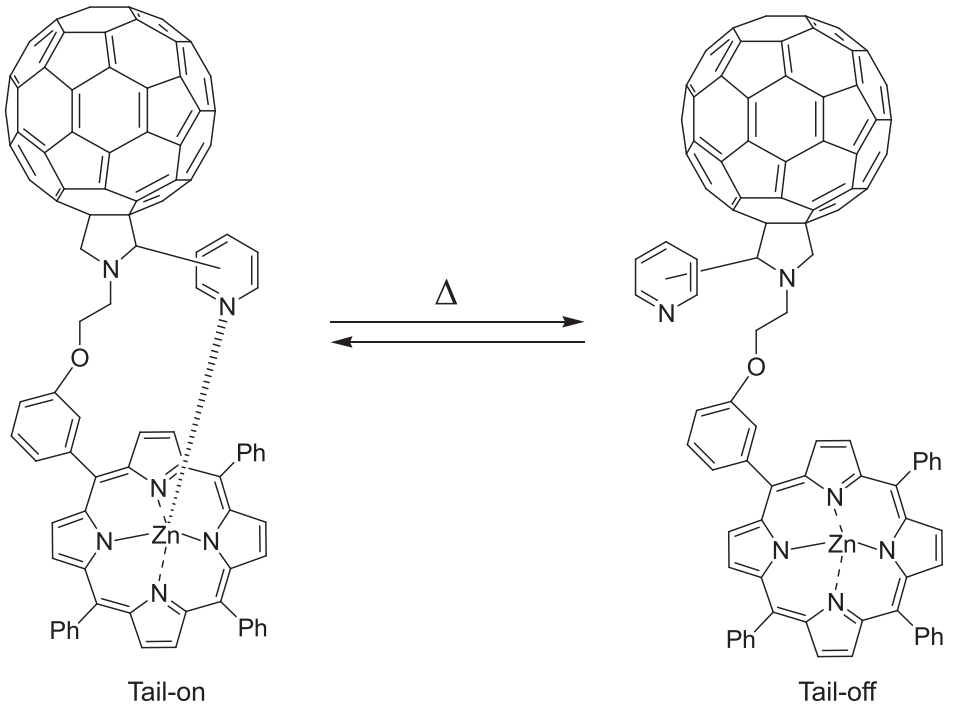

Figure 7. Temperature-dependent binding mechanism in the porphyrin-fullerene dyad.

was confirmed by single-crystal X-ray diffraction analysis and NMR.

Porphyrin nanobarrel **65** was prepared via the palladium-catalyzed Suzuki–Miyaura cross-coupling reaction. Initial tetraborylporphyrin **63** was treated with an excess of 2,6-dibromopyridine (Scheme 22) to yield tetra(6-bromopyridyl) porphyrin **64** whose following condensation with the starting porphyrin **63** afforded target product **65** in near 5% overall yield. Its composition was confirmed by mass-spectrometry (molecular formula $C_{232}H_{216}N_{24}Ni_4$), structure determination and refinement was based on the NMR and X-ray diffraction data. The inclusion complex hosting C_{60} was characterized by similar techniques (Figure 5).

Self-assembly of porphyrin-fullerene conjugates in water and organic solvents affords a variety of supramolecular architectures.[43-47]

5. Porphyrin-Fullerene Based Molecular Constructs

Very interesting behavior was reported for (1:1) inclusion complexes with fullerenes **67**, **68**, **69** hosted in porphyrin cyclic dimer **66** having a rather large cavity (Figure 6).[48]

The inclusion complex **66-67** based on Ru porphyrin dimer **66**[49] and nanocluster **67** composed of two C_{60} fullerenes[50] was formed via **66+67** self-assembly in toluene. The host-guest structure is characterized by the association constant of $8.4 \cdot 10^6$ M^{-1} and was shown to be formed at **66** to **67** ratio < 1. The inclusion complexes with **68** and **69** were produced analogously. Inclusion of fullerene nanocluster **67** with cyclic dimer **66** was demonstrated to induce axial oscillations of the π-electron density in the plane of **66**.

In comparing the ^{1}H NMR spectra (*i.e.* signals from *meso*-H and CH_3-Rh protons) at different temperatures it is apparent that guest **67** in complex **66-67** oscillates much faster than **68** and **69** counterparts. The oscillation frequency of **67** in **66-67** at 70° C is 1207 cycles per second. Oscillatory motion of the fullerene nanocluster within the host cavity depends upon the solvent, and its oscillation frequency reflects the solvation/desolvation dynamics of the fullerene, whose inclusion with porphyrin dimer **66** requires desolvation.

The above complex of cyclic Rh^{III} porphyrin dimer with C_{120} nanocluster is a new supramolecular oscillator that can find various applications in industry and science.

The porphyrin-fullerene dyad shown in Figure 7 exhibits the temperature-dependent binding mode (yielding "tail-on" or "tail-off" forms) that can be exploited to control the donor–acceptor proximity.[51] For the "tail-off" form the charge-separation efficiency was found to be somewhat higher compared to the "tail-on" form, suggesting the presence of some through-space interactions between the singlet excited Zn-porphyrin and the C_{60} moiety in the "tail-off" form.

Work[52] discusses the molecular logic devices based on using smart molecular systems for mimicking the function of logic gates, which constitute the basis of digital processing and computing (among recent developments are reconfigurable multiple logic gates in which single molecule performs multiple logic operations simultaneously). Of several diverse approaches to molecular logic, the photochemical concepts enjoy strong preference due to the ease with which changes in the optical output can be influenced through controlled excited state processes. Specifically, fluorescence switching between ON and OFF states based on photoinduced electron transfer (PET) is commonly implemented with molecular designs containing fluorophore–receptor conjugates, where the chemical input couples/decouples a PET-active fluorescent signaling unit from a receptor part and thus triggers/blocks PET-induced fluorescence quenching.

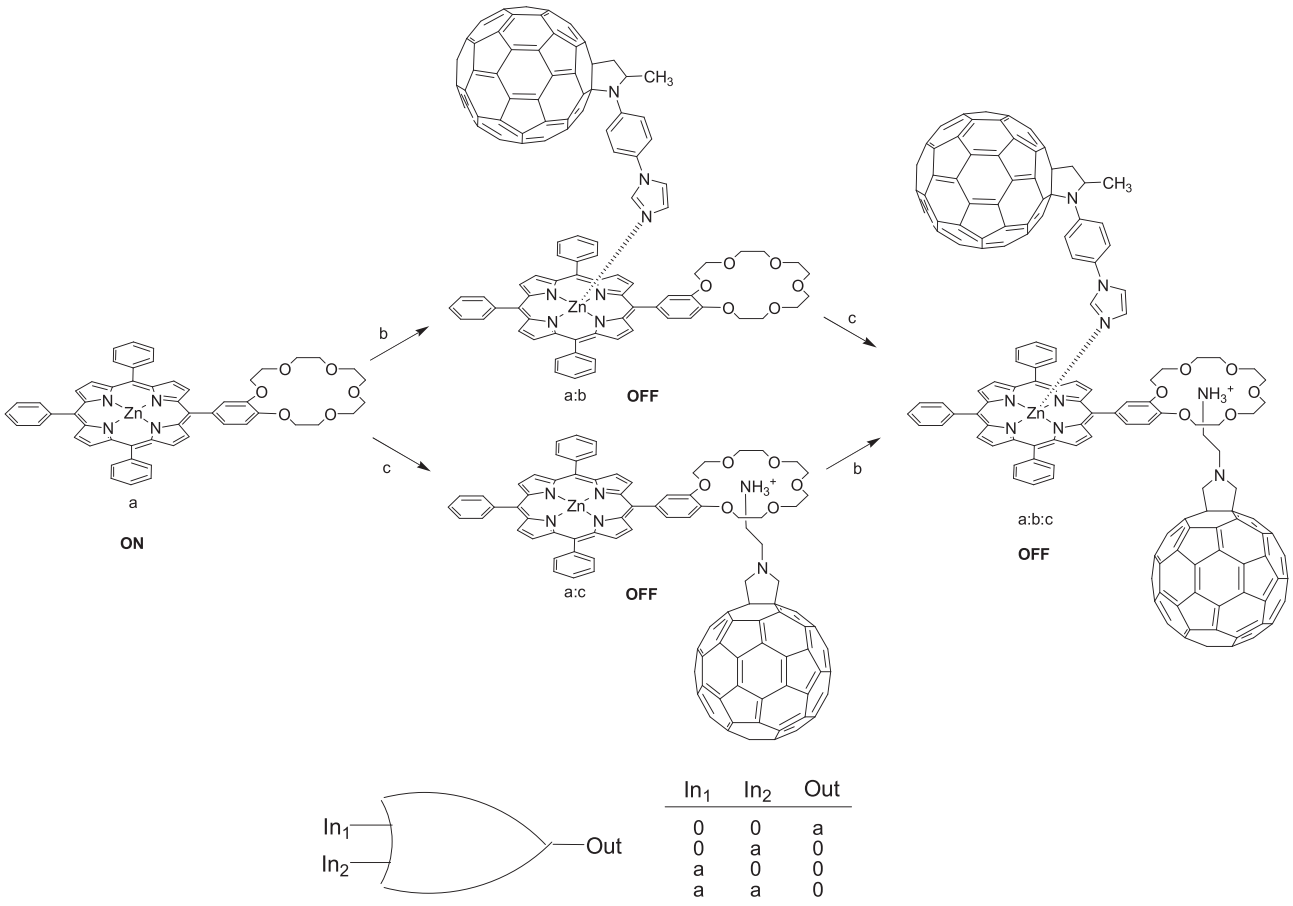

Figure 8. Construction of the NOR Logic Gate via a Self-Assembly Approach.

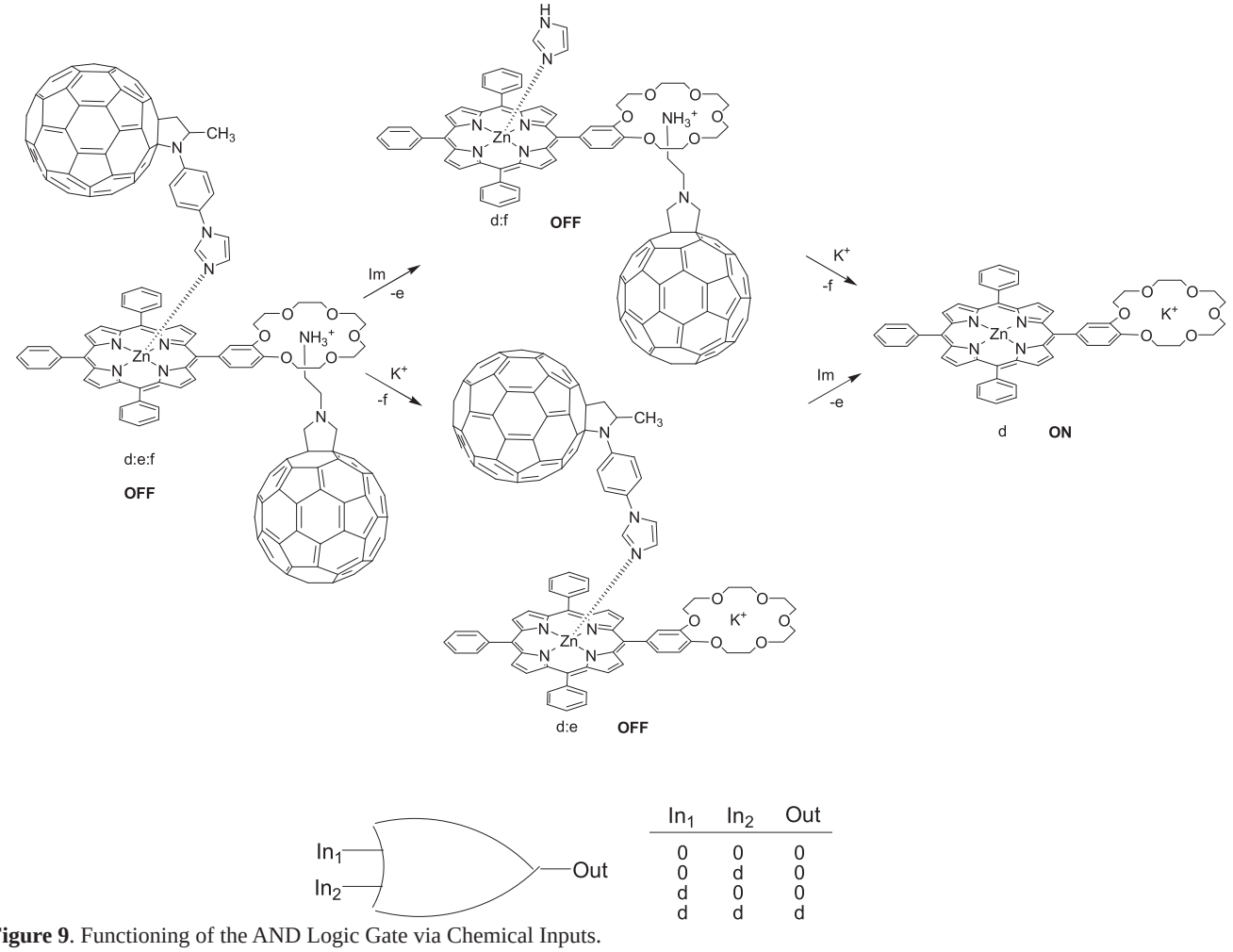

Figure 9. Functioning of the AND Logic Gate via Chemical Inputs.

The authors report the design of two-input NOR and AND molecular logic gates based on porphyrin-fullerene supramolecular arrays. The NOR function is mimicked by the Zn porphyrin linking to the two binding-site-selective C_{60} fullerene inputs either one of them (Figure 8). Benzo-18-crown-6 appended zinc porphyrin **a** in *o*-dichlorobenzene emits at 606 and 651 nm (excitation at the Soret band at 430 nm), that is ON state, and has two binding sites to attach C_{60}. The binding to phenylimidazole functionalized fullerene (in 1:1 ratio) via nitrogen–zinc coordination triggers PET-induced fluorescence quenching and results in the OFF state with zinc porphyrin fluorescence quenched by 70% (NOT operation). Analogously, adding equimolar amount of an alkyl ammonium functionalized fullerene which binds to the crown ether quenches 80% fluorescence (OFF state). Adding equimolar amounts of **b** and **c** to **a** gives the **a**:**b**:**c** complex practically not emitting fluorescence (> 90% quenching, OFF state). The resulting overall logic operation is NOR (each of receptor units as well as binding of both receptors gives rise to PET, which effectively quenches the fluorescence of Zn-porphyrin); the working principle of this NOR gate is illustrated in Figure 8.

Replacing the fullerene entities from the porphyrin–fullerene conjugate and restoring the original fluorescence by chemical inputs form the design basis of the AND logic gate (Figure 9). In this case, not-emitting **d:e:f** complex (OFF state) eliminates **e** fullerene unit on treatment with imidazole yielding **d:f** conjugate (still the OFF state). Adding of K^+ cation to **d:e:f** eliminates fullerene **f** giving not-emitting **d:e** conjugate (OFF state). Only the simultaneous addition of imidazole and K^+ to **d:e:f** leading to the loss of two fullerene units results in the ON state, that is, Zn porphyrin **d** emitting fluorescence (YES operation). The overall logic operation is AND: only when the both YES receptors are decoupled simultaneously, all possible PET pathways are blocked efficiently and the fluorescence output of the system is detected.

Thus, the above supramolecular architecture based on the combination of Zn-porphyrin with two functionalized C_{60} units can function as NOR or AND logic gate.

6. Potential Applications of Porphyrin-Fullerenes

The unique electronic properties of fullerenes and porphyrin-fullerenes make them excellent candidates for the development of optoelectronic and photovoltaic devices for diverse applications including medicine; much attention

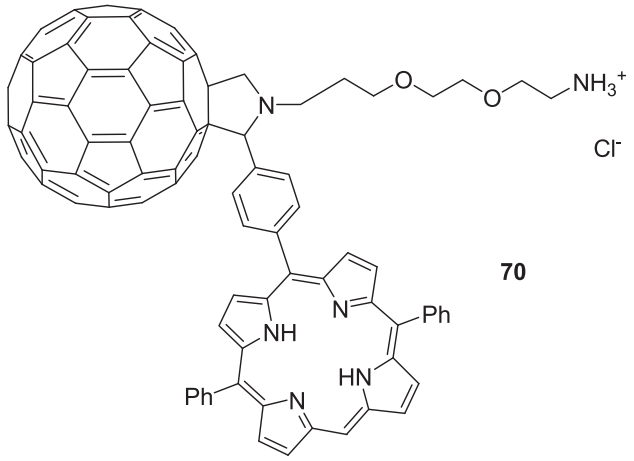

70

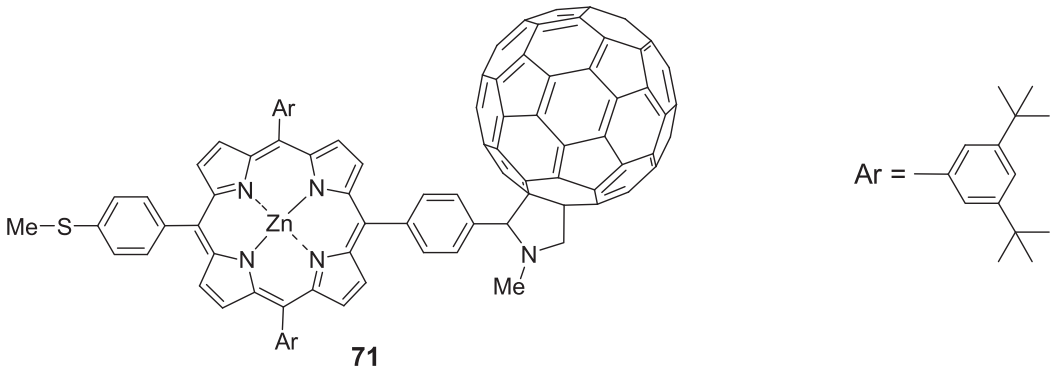

71

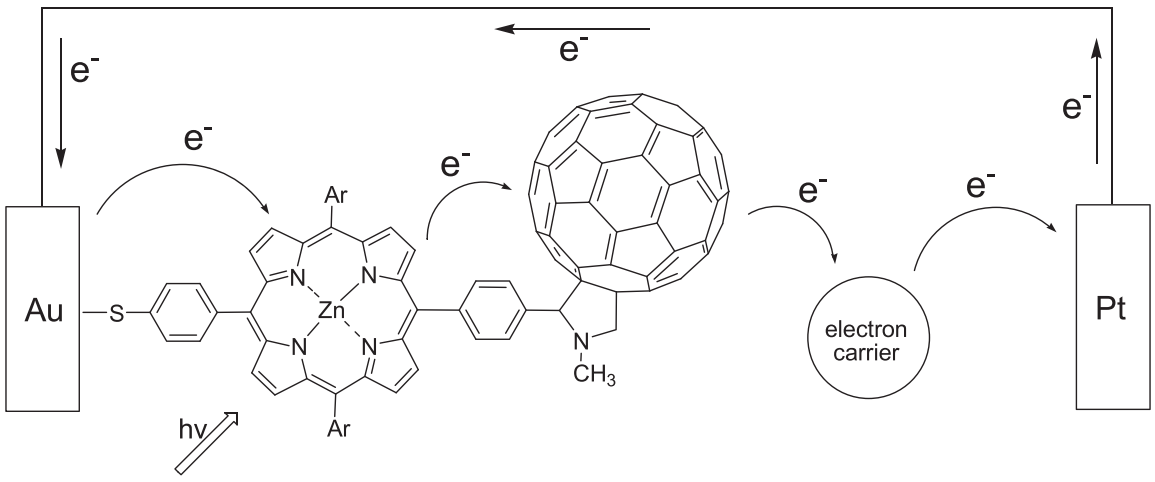

Figure 10. Photocurrent generation system based on gold electrodes with the monolayer porphyrin-fullerene coating.

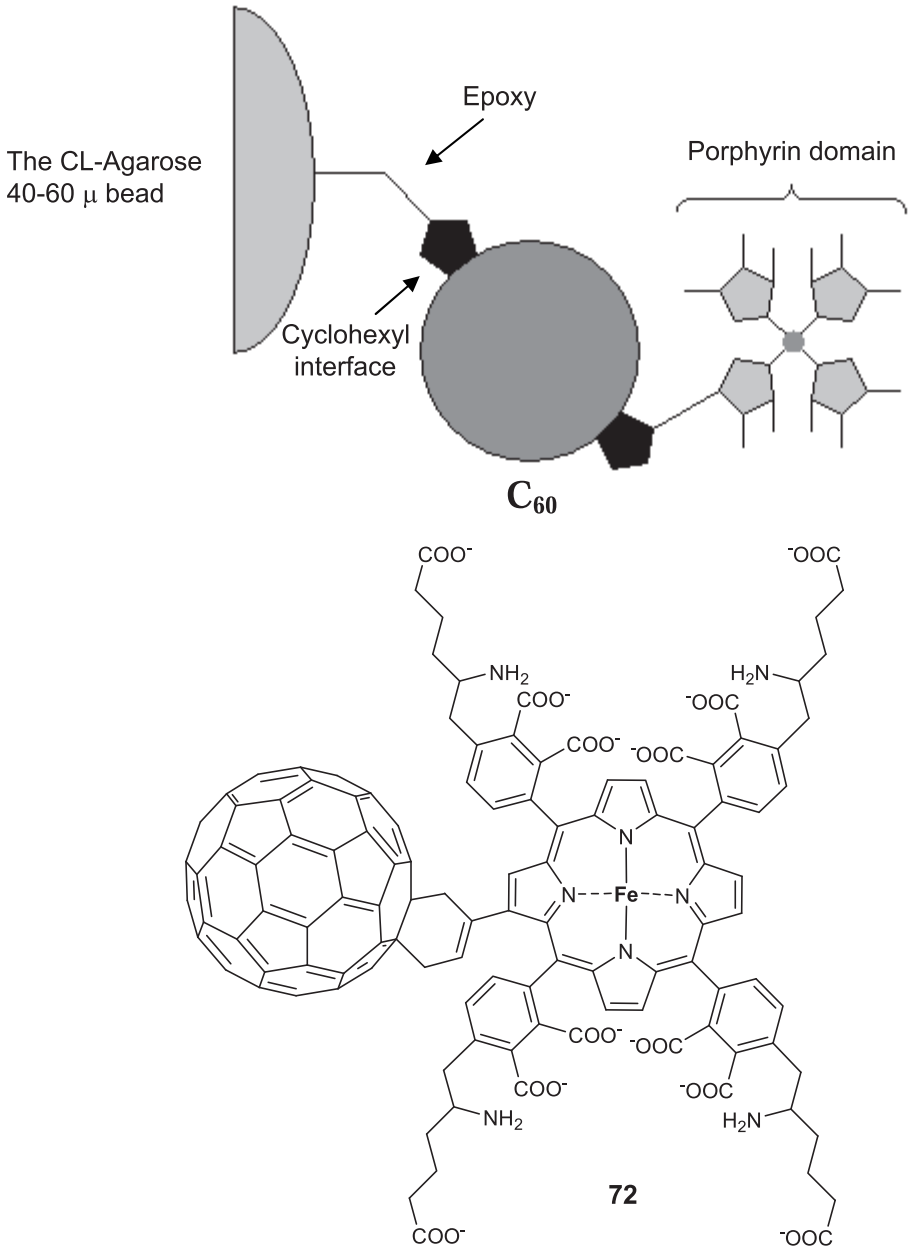

Figure 11. Stationary phase for purification of porphyrin binding proteins by affinity chromatography.

is also directed to the structural applications of porphyrin-fullerene systems, in particular for obtaining superhard and liquid crystal materials.

Among the recent developments are stable photoactive electrodes with a porphyrin–fullerene dyad **70** bearing the positively charged long-chain substituent.[53]

Importantly, in molecular photovoltaic systems the efficient PET step exhibited by porphyrin-fullerene complexes generally does not provide high photon-to-electron conversion efficiency which is as a necessary condition as the long-lived charge-separated state. When porphyrin-fullerene conjugates are affixed on electrodes for photocurrent generation, high photoconversion efficiencies can be realized, once the molecular orientation and energetics in such systems are optimized. Lipid bilayers and Langmuir–Blodgett films which are extensively used as the host of photosynthetic complexes lack the sufficient stability, are rather hard to handle, and put the upper limit of photon-to-electron conversion efficiency at about 10%. More promising showed the porphyrin-fullerene assembled monolayer structures immobilized on an electrode surface and in particular on the gold surface. Currently there is a considerable research interest in using this approach for a terminal conversion of light to photocurrent in solar devices, in catalytic applications etc.

Thus, the photocurrent generation system shown in Figure 10 is based on the gold electrode-supported porphyrin–fullerene dyad **71** assembled in a monolayer.[54]

The disulfide anchoring group of dyad **71** served to immobilize a self-assembled monolayer on a gold substrate. The more complex self-assembled systems of porphyrin-fullerene triads and tetrads were reported to be configured on electrodes into similar architectures. The effective photoconversion was observed for the ferrocene–Zn porphyrin–free-base porphyrin–C_{60} tetramer whose CS state lifetime reached 0.34 s.

The porphyrin-fullerene adduct anchored to the polysaccharide gel matrix has been used to chromatographically purify the mammalian cell membrane porphyrin binding proteins[55] Figure 11 shows the structure of conjugate **72** and (schematically) its linkage to hydroxyl groups on agarose. The pretreated protein fraction extracted from the rat myocardium mitochondria membranes was chromatographed on the porphyrin-fullerene-bound agarose gel column to isolate pure 17.6 kDa monomer protein composed of 122 amino acid residues.

Porphyrin-fullerene adduct **72** was used for targeted delivery of stable magnesium isotope $^{25}Mg^{2+}$ to the damaged heart muscle in rat models of myocardial hypoxia. Smart release of paramagnetic $^{25}Mg^{2+}$ isotope by ^{25}Mg-**72** nanocationite was shown to result in oxidative phosphorylation and ATP production increased 2.5 to 3.5-fold compared to nonmagnetic $^{26}Mg^{2+}$. As natural abundance of ^{25}Mg is 11%, the benefit of ^{25}Mg carrying porphyrin-fullerene is fairly apparent.[56]

The magnesium carrying porphyrin-fullerene nanoparticles reduce (by up to 70%) tolerance of myocardium for oxygen deficiency under conditions of cardiac failure, arrhythmia, physical activity, drug-induced cardiotoxicity.

The selected examples do not pretend to cover the wide field of all possible uses of porphyrin-fullerene structures. This unique class of organic compounds is holding great expectations and attracts intense interest and there is little doubt that future research will result in many more new applications.

7. References

1. Croto H.W., Heath J.R., O'Brien S.C., Curl R.F., Smalley R.F. C_{60}-Buckminsterfullerene. *Nature* **1985**, *318*, 162-163.
2. Prato M. Fulleropyrrolidines: a Family of Full-Fledged Fullerene Derivatives. *Acc. Chem. Res.* **1998**, *31*, 519-526.
3. Hirsch A. Principles of Fullerene Reactivity. *Top. Curr. Chem*. **1999**, *199*, 1-65.
4. Yurovskay M.A., Trushkov J.V. Cycloaddition to Buckminsterfullerene C_{60}: Advancements and Future Prospects. *Russ. Chem. Bull., Int. Ed.* **2002**, *51*, 367-443.
5. Mateo-Alonso A., Sooambar C., Prato M. *Org. Biomol. Chem.* **2006**, *4*, 1629-1637.
6. Martin N., Altable M., Filippone S., Martin-Domenech A. *Synlett* **2007**, *18*, 3077-3095.
7. Kharisov B.I., Kharisova O.B., Gomez M.J., Mendez U.O. Recent Advantages in Synthesis, Characterization, and Applications of Fulleropyrrolidines. *Int. Eng. Chem. Res.* **2009**, *48*, 545-571.
8. Sidorov L.N., Yurovskaya M.A., Borschevskii A.Y., Trushkov I.V., Ioffe I.N. *Fullerenes*. Moskva: Ekzamen. **2005**, 690 p. (in Russ.).
9. Hirsch A., Brettreich M., Wudl F. *Fullerene: Chemistry and Reactions.* Wiley-VCH: Weinhem, Germany, **2005**.
10. *Fullerenes: Principles and Applications* (Langa F., Nierengarten J.-F., Eds.), RSC Publishing: Cambridge, **2007**.
11. Abrasonis G., Amer M.S., Blanco R., Zhe C. *Fullerene Research Advances* (Kramer C.N., Ed.), Nova Sciences, **2007**.
12. Kordatos K., Bosi S., Dakos T., Zambon A., Lucchini V., Prato M. *J. Org. Chem.* **2001**, *66*, 2802-2808.
13. Marchesan S., Da Ros T., Prato M. *J. Org. Chem*. **2005**, *70*, 4706-4713.
14. Bourgeois J.P., Diederich F., Echegoyen L., Nierengarten J.-F. *Helv. Chim. Acta* **1998**, *81*, 1835-1844.
15. Armaroli N., Marconi G., Echegoyen L., Bourgeois J.-P., Diederich F. *Chem.-Eur. J.* **2000**, *6*, 1629-1645.
16. Armaroli N., Accorsi G., Song F.Y., Palkar A., Echegoyen L., Bonifazi D., Diederich F. *Chem. Phys. Chem*. **2005**, *6*, 732-743.
17. Bonifazi D., Scholl M., Song F.Y., Echegoyen L., Accorsi G., Armaroli N., Diederich F. *Angew. Chem., Int. Ed*. **2003**, *42*, 4969-4970.
18. Bonifazi D., Accorsi G., Armaroli N., Song F. Y., Palkar A., Echegoyen L., Scholl M., Seiler P., Jaun B., Diederich F. *Helv. Chim. Acta* **2005**, *88*, 1839-1884.
19. Accorsi G., Armaroli N. *J. Phys. Chem. C* **2010**, *114*, 1385-1403.
20. Spänig F., Kovacs Ch., Hauke F., Ohkubo K., Fukuzumi S., Guldi D.M., Hirsch A. *J. Am. Chem. Soc.* **2009**, *131*, 8180-8195.
21. Guldi D.M., Hirsch A., Scheloske M., Dietel E., Troisi A., Zerbetto F., Prato M. *Chem.-Eur. J.* **2003**, *9*, 4968-4979.
22. Hasobe T., Imahori H., Ohkubo K., Yamada H., Sato T., Nishimura Yo., Yamazaki I., Fukuzumi Sh. *J. Porphyrins Phthalocyanines* **2007**, *5*, 296-302.
23. Zheng G., Dougherty T.J., Pandey R.K. *Chem. Commun.* **1999**, 2469-2470.
24. Bell T.D.M., Ghiggino K.P., Haynes A., Hayenes A., Langford S.J., Woodward C.P. *J. Porphyrins Phthalocyanines* **2007**, *11*, 455-462.
25. Krutikova E.S., Bragina N.A., Mironov A.F. In: *Proceedings of the II International Youth School-Conference on Physical Chemistry of Crown Compounds, Porphyrins and Phthalocyanines*. **2010**, p. 56.
26. Gould S.L., Kodis G., Liddell P.A., Palacios R.E., Brune A., Gust D., Moore T.A., Moore A.L. *Tetrahedron* **2006**, *62*, 2074-2096.
27. Garg V., Kodis G., Chachisvilis M., Hambourger M., Moore A.L., Moore T.A., Gust D. *J. Am. Chem. Soc.* **2011**, *133*, 2944-2954.
28. Lembo A., Tagliatesta P., Cicero D., Leoni A., Salvatori A. *Org. Biomol. Chem.* **2009**, *7*, 1093-1096.
29. Hizume Y., Tashiro K., Charvet R., Yamamoto Y., Saeki A., Seki S., Aida T. *J. Am. Chem. Soc.* **2010**, *132*, 6628-6629.
30. Molina-Ontoria A., Wielopolski M., Gebhardt J., Gouloumis A., Clark T., Guldi D.M., Martin N. *J. Am. Chem. Soc.* **2011**, *133*, 2370-2373.
31. Kobori Y., Shibano Y., Endo T., Tsuji H., Murai H., Tamao K. *J. Am. Chem. Soc.* **2009**, *131*, 1624-1625.
32. Nierengarten J.-Fr. *J. Porphyrins Phthalocyanines* **2008**, *12*, 1022-1029.
33. Lindsey J.S., Wagner R.W. *J. Org. Chem.* **1989**, *54*, 828-836.
34. Guldi D.M. *Chem. Soc. Rev.* **2002**, *31*, 22-36.
35. Ohkubo K., Kotani H., Shao J., Ou Z., Kadish K.M., Li G., Pandey R.K., Fujitsuka M., Ito O., Imahori H., Fukuzumi S. *Angew. Chem., Int. Ed*. **2004**, *43*, 853-856.
36. Ohkubo K. In: *5th International Conference on Porphyrins and Phthalocyanines (ICPP-5). Book of Abstracts*. **2008**, Moscow, Russia, p. 45.
37. Mateo-Alonso A., Sooambar C., Prato M. *C.R. Chimia* **2006**, *9*, 944-951.
38. Poddutoori P.K., Sandanayaka A.S.D., Hasobe T. *J. Phys. Chem. A* **2010,** *114*, 11376-11385.
39. Santos L.J., Carvalho Da-Silva D., Reboucas J.S., Alves M.R.A,. Idemori Y.M., Matencio T., Freitas R.P., Alves R.B. *Tetrahedron* **2011**, *67*, 228-235.
40. Song J., Aratani N., Shinokubo H., Osuka, A. *J. Am. Chem. Soc*. **2010**, *132*, 16356-16357.
41. Jung S., Seo J., Shin S.K. *J. Phys. Chem. A* **2010**, *114,* 11376-11385.
42. Smith B.W., Monthioux M., Luzzi D.E. *Nature* **1998**, *396*, 323-324.

43. Hasobe T., Imahori H., Okhubo K., Yamada H., Sato T., Nishimura Y., Yamazaki I., Fukuzumi S. *J. Porphyrins Phthalocyanines* **2003**, *7*, 296-312.
44. Wolffs M., Hoeben F.J.M., Beckers E.H.A., Schenning A.P.H.J., Meijer E.W. *J. Am. Chem. Soc*. **2005**, *127,* 13484-13485.
45. Boyd P.D.W., *Hosseini* A., Rickard C.E.F. *Cryst. Growth Des.* **2006**, *6:2*, 397-403.
46. Hirofumi N., Fumito T., Yuichi S. *J. Phys. Chem. C* **2009**, *113,* 19694-19699.
47. Sandanayaka A.S.D., Murakami T., Hasobe T. *J. Phys. Chem. C* **2009**, *113*, 1839-18378.
48. Tashiro K., Hirabayashi Y., Aida T., Saigo K., Fujiwara K., Komatsu K., Sakamoto S., Yamaguchi *K. J. Am. Chem. Soc*. **2002,** *124*, 12086-12087.
49. Tashiro K., Aida T., Zheng J.-Y., Kinbara K., Saigo K., Sakamoto S., Yamaguchi K. *J. Am. Chem. Soc.* **1999**, *121*, 9477-9478.
50. Wang G.-W., Komatsu K., Murata Y., Shiro M. *Nature* **1997**, *387*, 583-586.
51. Maligaspe E., D'Souza F. *Org. Letters* **2010**, *12*, 624-627.
52. D'Souza F., Deviprasad G.R., El-Khouly M.E. Fujitsuka M., Ito O. *J. Am. Chem. Soc*. **2001**, *123,* 5277-5284.
53. Gournis D., Georgakilas V., Karakassides M.A., Bakas T., Kordatos K., Prato M., Fanti M., Zerbetto F. *J. Am. Chem. Soc*. **2004**, *126*, 8561-8568.
54. Imahori H., Mori, Y., Matano Y. *J. Photochem. Photobiol. C* **2003**, *4,* 51-83.
55. Amirshahi N., Alyautdin R.N., Rezayat S.M., Sarkar S., Orlova M.A., Orlov A.P., Poloznikov A.A., Kuznetsov D.A. *Chromatographia* **2008**, *68,* 295-298.
56. Sarkar S., Rezayat S.M., Buchachenko A.L., Sarkar S, Rezayat S.M., Buchachenko A.L., Kuznetsov D.A., Orlova M.A., Yurovskaya M.A. European Union Patents № 07009881.9 and № 07009882.7, **2007**, Munich, Germany.

Received 25.07.2011
Accepted 13.09.2011